究で行った電気鍼が単なる筋肉の電気刺激とは異なることが確認された。

次に、電気鍼を行う足の坐骨神経を剖出して切断の準備をした後、切断の前後で同じ電気鍼刺激を行って循環応答の変化を調べた（図9）。

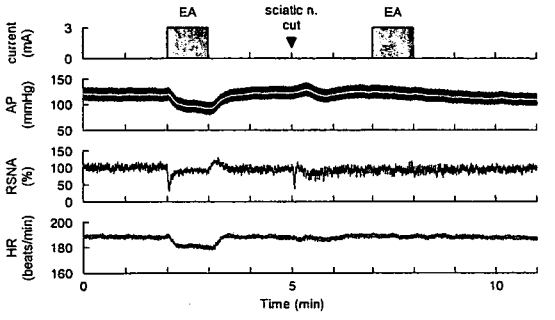

図９　坐骨神経（sciatic n.）切断前後での電気鍼（EA）に対する循環応答

その結果、坐骨神経の切除によって電気鍼（EA）に対する交感神経活動の抑制や血圧と心拍数の低下はみられなくなった。

Ｃ－５．麻酔ラットを用いた実験

ペントバルビタール麻酔ラットの足三里に電気鍼を行い、血圧応答を調べた。

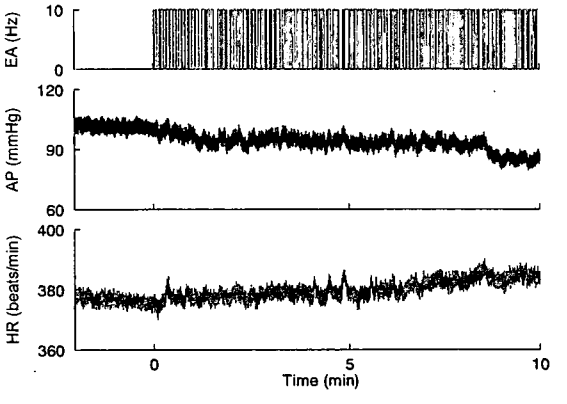

図１０　ラットにおける電気鍼に対する血圧と心拍数の応答の一例

図10は実験記録の一例である。ラットにおいても刺激部位を十分に探索すると、脛骨の外側部に電気鍼に応答する箇所がみられた。しかしながら、血圧応答の大きさはネコにみられた応答に比べて非常に小さかった。

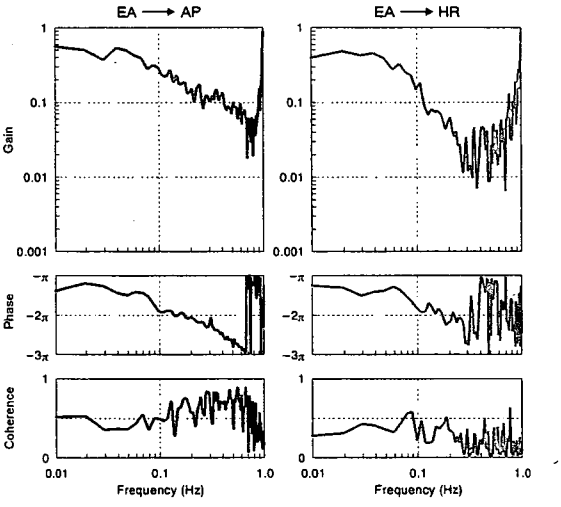

図１１　ラットにおける電気鍼から血圧応答までの伝達関数（EA→AP）および電気鍼から心拍数応答までの伝達関数（EA→HR）

図１１はラットにおける電気鍼から血圧応答までの伝達関数と電気鍼から心拍数応答までの伝達関数を示したものである。いずれも高周波になるほど応答が小さくなる低域通過フィルターの性質を示したが、伝達関数のゲインはネコのそれに比べて約1/10であった。このため、入出力関係の線形性の指標となるコヒーレンスも血圧応答で約0.5、心拍数応答ではそれよりも小さかった。

Ｄ．考察

麻酔下のネコにおいて、電気鍼刺激は交感神経活動抑制、血圧低下、心拍数低下作用を示した。本研究では動脈圧反射をつかさどる圧受容器や、心肺受容器からの求心路である迷走神経を切除しない状態で実験を行っているので、これらの反射系は電気鍼刺激の効果を打ち消すように作用すると考えられる。それにも関わらず、電気鍼刺

激に対する血圧応答の伝達関数のゲインが約 10 であることは、1 mA の刺激で血圧が約 10 mmHg 変化したことを意味しており、電気鍼刺激が強力な血圧低下作用を持つことを示唆する（図 1)。

本年度は電気鍼から血圧応答までの伝達関数の数学モデルを利用して、フィードバックによって電気鍼の強度を調節するシステムを設計し、その性能を評価した。前年度の研究結果から、電気鍼の効果は電流強度に応じて大きくなることが分かっていたので、当初は電流強度だけを操作量とする比例-積分型制御装置を作成し、電気鍼による血圧制御を行った。その結果、刺激電流に対する血圧応答が非常に大きな個体において、刺激閾値の前後で電気鍼の刺激コマンドと血圧応答が発振現象を示す場合があった（図 4)。このような問題を回避するために、刺激コマンドが 1 より小さいときは、電流強度を 1 mA に固定して、刺激周波数を低下させることで血圧を制御できるように制御装置を改良した。その結果、非常に弱い電流強度で血圧が十分に低下する個体においても、発振現象を起こすことなく血圧が制御できるようになった（図 5)。この制御装置を用いることで、1 分以内に血圧をちょうど 20 mmHg だけ低下することが可能であり、制御の間、安定した血圧を保つことが可能であった（図 6)。このとき、血圧値が非常に狭い範囲で制御されたのに対して、電気鍼の刺激コマンドには大きな個体差が生じた。これは、電気鍼に対する血圧応答が大きい個体では刺激コマンドが自動的に小さくなり、電気鍼に対する血圧応答が小さい個体では刺激コマンドが自動的に大きくなるようにフィードバック制御された結果である。したがって、本システムを用いることで電気鍼に対する血圧応答の個体差に関係なく、安定して血圧が制御できるようになった。

電気鍼に際して血圧の低下とともに腎臓交感神経の低下が観察されたことから、本研究で行った電気鍼が中枢を介するものであることは間違いないが、さらに求心路を明らかにするために 2 つの実験を行った。1 つめは下腿三頭筋の電気刺激実験である（図 8)。電気鍼に使用したのと同じ強度（3 mA）で下腿三頭筋を電気刺激したところ、電気刺激に応じた筋肉の収縮は観察されたが、この筋肉の収縮が血圧の低下や腎臓交感神経活動の低下を起こすことはなかった。したがって、本研究で行った電気鍼に対する循環応答は、筋肉の機械的収縮によって惹起されたものではないことが確認された。2 つめは坐骨神経の切断実験である（図 9)。電気鍼を行った足と同側の坐骨神経を切断することによって、電気鍼に対する循環応答は消失した。このことから、本研究で行った電気鍼が神経経由で循環応答を惹起していることが確認された。

最後に、麻酔ネコで確立した方法を麻酔ラットに適用して、電気鍼に対する血圧および心拍数応答の動特性を調べた。麻酔ラットでは麻酔ネコに比べて循環応答がみられるツボの探索に時間を要した。また、電気鍼に対する血圧応答もネコのそれに比べて約 1/10 であり、電気鍼に対する循環応答の種差が示唆された。

E．結論

工学の分野で広く用いられている白色雑音法を用いて、電気鍼刺激に対する動的な

循環応答を定量化することが可能であった。これまでに、このような定量的な解析は実施されていないことから、本研究結果は電気鍼を用いた循環器疾患に対する新たな治療システムの開発に大きく貢献すると期待される。

本年度は適切なフィードバックによる電気鍼システムのための最適な制御系を設計し、それを実時間で駆動できるソフトウェアを開発し、実際に制御の性能を動物実験で確認した。その結果、電流強度と刺激周波数を同時に制御することによって、1 分以内に 20 mmHg の降圧効果を発揮できるような電気鍼システムを開発することが可能であった。このようなシステムの開発の枠組みが完成したことから、今後は病態モデルにおける治療実験を行うために、同様のシステムをラットなどの小動物で構築していく必要がある。

F．健康危険情報

なし

G．研究発表

G－1．論文

1. Regional difference in ischaemia-induced myocardial interstitial noradrenaline and acetylcholine releases. Kawada T, Yamazaki T, Akiyama T, Shishido T, Shimizu S, Mizuno M, Mori H, Sugimachi M. Auton Neurosci 137: 44-50, 2007.
2. Angiotensin II attenuates myocardial interstitial acetylcholine release in response to vagal stimulation. Kawada T, Yamazaki T, Akiyama T, Li M, Zheng C, Shishido T, Mori H, Sugimachi M. Am J Physiol Heart Circ Physiol 293: H2516-H2522, 2007.

G－2．学会発表

1. 川田　徹、山崎　登自、秋山　剛、宍戸　稔聡、神谷　厚範、水野　正樹、杉町　勝．アンジオテンシンⅡは迷走神経刺激時の心筋間質におけるアセチルコリン放出を抑制する．第 84 回日本生理学会大会　Program2007
2. 川田　徹、上村　和紀、宍戸　稔聡、杉町　勝　小動物における Bluetooth 圧容積テレメトリの試作．第 46 回日本生体工学会大会
3. 清水　秀二、宍戸　稔聡、上村　和紀、神谷　厚範、杉町　勝．Norwood 手術のシャント術式が心臓エナジェティクスに与える影響．第 46 回日本生体工学会大会
4. 宮本　忠吉、稲垣　正司、高木　洋、川田　徹、宍戸　稔聡、神谷　厚範、杉町　勝．ヒト呼吸化学調節系の動特性の定量評価．第 46 回日本生体工学会大会
5. 杉町　勝、上村　和紀、神谷　厚範、清水　秀二、宍戸　稔聡、砂川　賢二．包括循環平衡モデルに基づくバイオニック循環管理．第 28 回日本循環制御医学会総会
6. 李　梅花、鄭　燦、川田　徹、稲垣　正司、宍戸　稔聡、佐藤　隆幸、杉町　勝．アセチルコリンエステラーゼ阻害薬ドネペジルは心筋梗塞後ラットの心臓リ

モデリングと心機能低下を防止する. 第28回日本循環制御医学会総会

7. Li M, Zheng C, Kawada T, Inagaki M, Shishido T, Sato T, Sugimachi M. Restoration of vagal tone by donepezil markedly improves long-term survival in rats with incurably severe heart failure. EXRERIMENTAL BIOLOGY 2007
8. Shimizu S, Shishido T, Uemura K, Kamiya A, Kawada T, Sano S, Sugimachi M. Right ventricle-pulmonary artery shunt for Norwood procedure is beveficial in reducing pressure-volume area and myocardial oxygen consumption compared to Blalock-Taussing Shunt: an in-silico analysis. European Society of Cardiology 2007
9. 水野　正樹、神谷　厚範、川田　徹、宍戸　稔聡、杉町　勝. ムスカリン性K+チャネルは交感神経緊張の有無に関わらず迷走神経刺激に対する動的及び静的心拍応答に貢献している. 第85回日本生理学会総会
10. 川田　徹、水野　正樹、神谷　厚範、宍戸　稔聡、杉　町勝. 血圧フィードバックによる電気鍼を用いた交感神経抑制システムの開発. 第85回日本生理学会総会
11. Li M, Inagaki M, Zheng C, Kawada T, Uemura K, Shishido T, Sato T, Sugimachi M. Both acute and chronic-phase vagal stimulation markedly suppressed arrhythmic death and prevented remodeling in rats after large myocardial infarction. The 72nd Annual Scientific Meeting of the Japanese Circulation Society
12. Li M, Zheng C, Kawada T, Inagaki M, Shishido T, Sato T, Sugimachi M. Addition of acetylcholinesterase inhibitor, donepezil improves neurohumoral states further than losartan alone in rats with extensive myocardial infarction. The 72nd Annual Scientific Meeting of the Japanese Circulation Society
13. Une D, Shimizu S, Shishido T, Yoshitaka H, Sugimachi M, Kuinose M. Variable flow of successful LITA graft for proximal LAD lesion can be almost exclusively explained by double product. The 72nd Annual Scientific Meeting of the Japanese Circulation Society

H．知的所有権の取得状況

なし

研究成果の刊行に関する一覧表

書籍

著者名	論文タイトル	書籍全体の編集者名	書籍名	出版社名	出版地	出版年	ページ
川田 徹	圧受容器反射	熊谷裕生, 小室一成, 堀内正嗣, 森下竜一	高血圧ナビゲーター第2版	メディカルレビュー社	東京	2008	138-9

雑誌

発表者氏名	論文タイトル名	発表誌名	巻号	ページ	出版年
Yamazaki T, Akiyama T, Kitagawa H, Komaki F, Mori H, Kawada T, Sunagawa K, Sugimachi M	Characterization of ouabain-induced noradrenaline and acetylcholine release from in situ cardiac autonomic nerve endings	Acta Physiol (Oxf)	191	275-84	2007
Uemura K, Li M, Tsutsumi T, Yamazaki T, Kawada T, Kamiya A, Inagaki M, Sunagawa K, Sugimachi M	Efferent vagal nerve stimulation induces tissue inhibitor of metalloproteinase-1 in myocardial ischemia-reperfusion injury in rabbit	Am J Phsyiol Heart Circ Physiol	293	H2254-61	2007
Kawada T, Yamazaki T, Akiyama T, Shishido T, Shimizu S, Mizuno M, Mori H, Sugimachi M	Regional difference in ischemia-induced myocardial interstitial noradrenaline and acetylcholine releases	Auton Neurosci: Basic and Clinical	137	44-50	2007
Kawada T, Yamazaki T, Akitama T, Li M, Zheng C, Shishido T, Mori H, Sugimachi M	Angiotensin II attenuates myocardial interstitial acetylcholine release in response to vagal stimulation	Am J Physiol Heart Circ Physiol	293	H2516-22	2007
Mizuno M, Kamiya A, Kawada T, Miyamoto T, Shimizu S, Sugimachi M	Muscarinic potassium channels augment dynamic and static heart rate response to vagal stimulation	Am J Physiol Heart Circ Physiol	293	H1564-70	2007
Kawada T, Kitagawa H, Yamazaki T, Akitama T, Kamiya A, Uemura K, Mori H, Sugimachi M	Hypothermia reduces ischemia- and stimulation-induced myocardial interstitial norepinephrine and acetylcholine releases	J Appl Physiol	102	622-627	2007

Am J Physiol Heart Circ Physiol 293: H2254–H2261, 2007.
First published August 10, 2007; doi:10.1152/ajpheart.00490.2007.

Efferent vagal nerve stimulation induces tissue inhibitor of metalloproteinase-1 in myocardial ischemia-reperfusion injury in rabbit

Kazunori Uemura,[1] Meihua Li,[1] Takaki Tsutsumi,[2] Toji Yamazaki,[3] Toru Kawada,[1] Atsunori Kamiya,[1] Masashi Inagaki,[1] Kenji Sunagawa,[2] and Masaru Sugimachi[1]

Departments of [1]Cardiovascular Dynamics and [3]Cardiac Physiology, National Cardiovascular Center Research Institute, Suita, Japan; and [2]Department of Cardiovascular Medicine, Kyushu University Graduate School of Medical Science, Fukuoka, Japan

Submitted 24 April 2007; accepted in final form 7 August 2007

Uemura K, Li M, Tsutsumi T, Yamazaki T, Kawada T, Kamiya A, Inagaki M, Sunagawa K, Sugimachi M. Efferent vagal nerve stimulation induces tissue inhibitor of metalloproteinase-1 in myocardial ischemia-reperfusion injury in rabbit. *Am J Physiol Heart Circ Physiol* 293: H2254–H2261, 2007. First published August 10, 2007; doi:10.1152/ajpheart.00490.2007.—Vagal nerve stimulation has been suggested to ameliorate left ventricular (LV) remodeling in heart failure. However, it is not known whether and to what degree vagal nerve stimulation affects matrix metalloproteinase (MMP) and tissue inhibitor of MMP (TIMP) in myocardium, which are known to play crucial roles in LV remodeling. We therefore investigated the effects of electrical stimulation of efferent vagal nerve on myocardial expression and activation of MMPs and TIMPs in a rabbit model of myocardial ischemia-reperfusion (I/R) injury. Anesthetized rabbits were subjected to 60 min of left coronary artery occlusion and 180 min of reperfusion with (I/R-VS, $n = 8$) or without vagal nerve stimulation (I/R, $n = 7$). Rabbits not subjected to coronary occlusion with (VS, $n = 7$) or without vagal stimulation (sham, $n = 7$) were used as controls. Total MMP-9 protein increased significantly after left coronary artery occlusion in I/R-VS and I/R to a similar degree compared with VS and sham values. Endogenous active MMP-9 protein level was significantly lower in I/R-VS compared with I/R. TIMP-1 mRNA expression was significantly increased in I/R-VS compared with the I/R, VS, and sham groups. TIMP-1 protein was significantly increased in I/R-VS and VS compared with the I/R and sham groups. Cardiac microdialysis technique demonstrated that topical perfusion of acetylcholine increased dialysate TIMP-1 protein level, which was suppressed by coperfusion of atropine. Immunohistochemistry demonstrated a strong expression of TIMP-1 protein in cardiomyocytes around the dialysis probe used to perfuse acetylcholine. In conclusion, in a rabbit model of myocardial I/R injury, vagal nerve stimulation induced TIMP-1 expression in cardiomyocytes and reduced active MMP-9.

myocardial remodeling; matrix metalloproteinase; acetylcholine

LEFT VENTRICULAR (LV) myocardial remodeling that occurs after myocardial infarction (MI) leads to progressive LV dilation and eventually pump dysfunction (33, 40). In addition to the loss of contractile cardiomyocytes, pathological degradation and reconstitution of extracellular matrix significantly contribute to the progression of LV remodeling, where matrix metalloproteinase (MMP) and its intrinsic inhibitor, tissue inhibitor of MMP (TIMP), play crucial roles (37, 43).

A previous study using genetically engineered mice demonstrated that target deletion of the MMP-9 gene prevented LV rupture and ameliorated LV remodeling after MI (10). The positive results of MMP inhibition on LV remodeling in animal models led to the proposal to use MMP inhibitors as a potential therapy for patients at risk for the development of heart failure after MI (27, 32). However, recent clinical results from the Prevention of Myocardial Infarction Early Remodeling (PREMIER) trial failed to demonstrate a beneficial effect of MMP inhibition on LV remodeling after MI (16). This indicates the importance of further understanding the in vivo regulatory mechanisms of MMPs to understand and beneficially modify the LV remodeling process.

The cardiac autonomic nervous system plays an important role in the progression of heart failure (21). A previous communication from our laboratory demonstrated that chronic electrical stimulation of vagal nerve ameliorated LV remodeling and markedly improved survival after MI in rat (23). However, it is not known whether and to what degree the vagal nerve affects the MMPs and the TIMPs in vivo. We therefore investigated the effects of electrical stimulation of vagal nerve on myocardial expression of MMP-2/9 and TIMP-1/2 in a rabbit model of myocardial ischemia-reperfusion (I/R) injury. We also investigated the direct action of acetylcholine (ACh), a neurotransmitter released by vagal nerve stimulation (VNS), on myocardial release of TIMP-1 using a cardiac microdialysis technique (19). Our results indicated that VNS induced expression of TIMP-1 from cardiomyocytes and reduced active MMP-9 in myocardial I/R injury in rabbit.

METHODS

We used 49 Japanese white rabbits in this study (male, 2.5–3.0 kg). Care of the animals was in strict accordance with the guiding principles of the Physiological Society of Japan. All protocols were approved by the Animal Subjects Committee of the National Cardiovascular Center.

I/R Study

Experimental preparation. Anesthesia was induced by intravenous injection of pentobarbital sodium (35 mg/kg). Animals were tracheotomized, intubated, and mechanically ventilated. Arterial pH, P_{O_2}, and P_{CO_2} were maintained within the physiological ranges by supplying oxygen and changing the respiratory rate. α-Chloralose (20 $mg \cdot kg^{-1} \cdot h^{-1}$) was continuously infused to maintain an appropriate level of anesthesia during the experiment. A catheter-tipped micromanometer (SPC-330A, Millar Instruments, Houston, TX) was inserted via the right femoral artery to measure arterial pressure (AP). After a median sternotomy, the heart was suspended in a pericardial

Address for reprint requests and other correspondence: K. Uemura, Dept. of Cardiovascular Dynamics, National Cardiovascular Center Research Inst., 5-7-1 Fujishirodai, Suita 565-8565, Japan (e-mail: kuemura@ri.ncvc.go.jp).

The costs of publication of this article were defrayed in part by the payment of page charges. The article must therefore be hereby marked "*advertisement*" in accordance with 18 U.S.C. Section 1734 solely to indicate this fact.

cradle. Another catheter-tipped micromanometer was introduced into the LV via the apex to measure LV pressure (LVP). Piezoelectric crystals (1 mm, Sonometrics, Ontario, Canada) were attached to the anterior and lateral walls of the LV using cyanoacrylate adhesive (3M, Vetbond, St. Paul, MN) to measure regional LV segmental length. A 4-0 proline suture was passed around the main branch of the left anterior descending coronary artery (LAD), and a snare was formed by passing the ends of the thread through a small vinyl tube. A surface electrocardiogram (ECG) was recorded.

Bilateral cervical vagi were identified and transected at the neck region. A pair of bipolar electrodes was attached at the cardiac end of the right vagal nerve. The duration of electrical pulse used to stimulate the vagal nerve was set at 4 ms. We adjusted the amplitude of the pulse in each animal to reduce heart rate (HR) by 30% from the baseline value at a stimulation frequency of 10 Hz. The resultant stimulation voltage was 2–4 V.

Experimental protocol. Thirty minutes were allowed for stabilization after the initial preparation and surgical procedures were completed. The animals were randomized into the following four groups: *1*) sham group (n = 7), in which surgical preparation was conducted without coronary occlusion or vagal stimulation (VS); *2*) VS group (n = 7), in which stimulation of the vagal nerve was started after baseline hemodynamics were obtained and continued during the experiment; *3*) I/R group (n = 7), in which 60 min of LAD occlusion and 180 min of reperfusion were conducted; and *4*) I/R-VS group (n = 8), in which stimulation of the vagal nerve was started 15 min before LAD occlusion and continued throughout 60 min of myocardial ischemia and 180 min of reperfusion.

Baseline hemodynamic data (baseline) were recorded in all groups. A second set of measurements of hemodynamic data (60 min) was obtained during the last 5 min of the 60-min observation period in the sham and VS groups or during the last 5 min of the 60-min ischemic period in the I/R and I/R-VS groups. A third set of measurements of hemodynamic data (240 min) was recorded during the last 5 min of the next 180-min observation period in the sham and VS groups or during the last 5 min of the 180-min reperfusion period in the I/R and I/R-VS groups.

At each time point, hemodynamic data were recorded under a steady-state condition. All data acquisitions were done at end expiration. Analog signals of AP, LVP, segmental length of the anterior-lateral wall of LV (risk area), and ECG were digitized at 200 Hz and stored in a computer for off-line analysis (Sonolab, Sonometrics).

At the end of the experiment, the animal was euthanized. The whole heart was quickly excised and washed with cold PBS. After the vasculature, right ventricular free wall, and atrial appendages were dissected away, the remaining LV wall was snap frozen in liquid nitrogen and stored at −80°C.

Myocardial protein extraction. Approximately 200 mg of myocardial tissue sample obtained from the center of the risk area (anterior wall) of the LV free wall was homogenized in 1 ml of lysis buffer containing 50 mmol/l Tris (pH 7.4), 1.5 mmol/l $CaCl_2$, and 0.5% Triton X-100. The homogenate was centrifuged at 2,000 *g* for 10 min at 4°C, and the supernatant was collected. Protein concentration of each supernatant sample was determined with a DC Protein assay kit (Bio-Rad, Richmond, CA).

Gelatin zymography. Gelatin zymography was performed to assess the relative contents of the gelatinases MMP-2 and MMP-9 (43). The supernatants (60 μg protein) were loaded in Novex precast 10% Tris-glycine gels containing 0.1% gelatin (Invitrogen, Carlsbad, CA) and then electrophoresed. After renaturation and equilibration, the gels were incubated for 30 h at 37°C in Novex zymogram-developing buffer. The gels were then stained in 0.5% Coomassie blue G-250, dissolved in 30% methanol-10% acetic acid for 60 min, and destained in several changes of methanol-acetic acid for 60 min. Gels were dried and scanned. MMP-2 and MMP-9 related bands were analyzed using the NIH Image software (ImageJ 1.37).

MMP-9 activity assay. Bioactivity assay for MMP-9 was performed using the Biotrak activity assay system (GE Healthcare Bio-Sciences, Piscataway, NJ) following the manufacturer's instructions (42). Briefly, supernatant samples were placed in microtitre well plates coated with anti-MMP-9 (100 μl/well). The plates were incubated overnight at 4°C. The following day, *p*-aminophenylmercuric acetate was added to the wells for measuring "total" MMP-9 (pro- and active MMP-9). Buffer alone was added to the wells for measuring "active" (endogenous active MMP-9) MMP-9. Detection agent was then added to all wells (50 μl/well), and the plate was read at 405 nm (t = 0 min) and again after a 2-h incubation at 37°C. The value of MMP-9 was standardized by the protein concentration. All measurements were run in duplicate.

ELISA measurement of TIMP-1 and TIMP-2. Commercially available ELISA kits (Daiichi Fine Chemical, Toyama, Japan) were used to measure TIMP-1 and TIMP-2 levels in supernatants according to the manufacturer's instructions (13, 17, 20). Briefly, standards and samples were incubated in microtitre wells coated with anti-TIMP-1 and anti-TIMP-2 antibody. Peroxidase-labeled antibodies directed to the respective TIMPs were added to the corresponding wells. Visualization of the presence of the peroxidase label was achieved using the *o*-phenylenediamine substrate (TIMP-1) or tetramethylbenzidine substrate (TIMP-2). The plates were read at 490 (TIMP-1) or 450 (TIMP-2) nm. Values of TIMPs were standardized by the protein concentration. Since the ELISA systems have some degree of intraplate and interplate variability (<15%) (7), all measurements were run in duplicate to quadruplicate.

Myocardial RNA extraction and reverse transcription. Total RNA was extracted from the risk area (anterior wall) of the LV free wall by an acid guanidium thiocyanate-phenol chloroform method (Isogen, Nippon Gene). First-strand cDNA was synthesized using reverse transcriptase with random hexamer primers from 1 μg of total RNA in a final volume of 20 μl, according to the manufacturer's protocol (ReverTra Ace, Toyobo).

Real-time quantitative reverse transcription-PCR. To analyze TIMP-1 gene expression in myocardial tissue, real-time polymerase chain reaction (PCR) amplification was performed with SYBR Premix Ex Taq (Perfect Real Time; TaKaRa, Japan) using the ABI PRISM 7500 sequence detection system (Applied Biosystems). For standardization and quantification, rabbit glyceraldehyde 3-phosphate dehydrogenase (GAPDH) was amplified simultaneously. The respective PCR primers were designed from GenBank databases (Table 1). The PCR consisted of initial treatments (50°C, 2 min; and 95°C, 10 min) followed by 40 three-step cycles (denaturation 94°C, 10 s; annealing 60°C, 10 s; and extension 72°C, 40 s). Fluorescence was detected at the end of every extension phase (72°C). After PCR amplification, dissociation curves were constructed to confirm the formation of the intended PCR products. Relative expression of TIMP-1 to the GAPDH levels was calculated as described previously (28, 45).

Hemodynamic data analysis. The following hemodynamic parameters were determined from hemodynamic data: HR, mean arterial pressure, maximum first derivative of LVP (LV dP/dt_{max}), and fractional shortening of anterior-lateral wall (FS). End diastole and end ejection were defined as the peak of R wave of ECG and the peak of minimum first derivative of LVP, respectively. FS was calculated as

Table 1. *Probes used for real-time PCR*

Assay	Sequence	Accession Number
TIMP-1		
Forward	5′-CAACTCCGACCTTGTCATCAG-3′	AY829731
Reverse	5′-GCGTCAAATCCTTTGAACATCT-3′	
GAPDH		
Forward	5′-GGAGAAAGCTGCTAAGTATGACG-3′	L23961
Reverse	5′-CACTGTTGA AGTCGCAGGAG-3′	

TIMP-1, tissue inhibitor of matrix metalloproteinase-1.

the ratio of systolic stroke change in segmental length and end-diastolic length of the anterior-lateral wall (36).

Cardiac Microdialysis Study

Experimental preparation. Experimental preparation was the same as described above in *I/R Study*, except that no coronary artery occlusion was performed. A microdialysis probe was implanted into the LV anterior wall. Heparin sodium (200 U/kg) was administered intravenously to prevent blood coagulation (19).

Dialysis technique. The materials and properties of the dialysis probe have been described (19). Briefly, we designed a hand-made long transverse dialysis probe. One end of a polyethylene tube (25 cm long, 0.5 mm OD, and 0.2 mm ID) was dilated with a 27-gauge needle (0.4 mm OD). Each end of the dialysis fiber (8 mm long, 0.215 mm OD, 0.175 mm ID, and 300 Å pore size; Evaflux type 5A, Kuraray Medical, Tokyo, Japan) was inserted into the polyethylene tube and glued.

Recovery of TIMP-1 passing through the dialysis fiber membrane was evaluated in vitro. The dialysis probe ($n = 4$) was immersed in Ringer solution (in mM; 147.0 NaCl, 4.0 KCl, and 2.25 $CaCl_2$) containing Tween 20 (0.1%) and various concentrations of TIMP-1 (10–40 ng/ml, free form of human TIMP-1, Daiichi Fine Chemical). The dialysis probe was perfused with Ringer solution at a rate of 2.5 μl/min using a microinjection pump (model CMA/102, Carnegie Medicine). We measured the concentration of TIMP-1 in the dialysate sample using an ELISA kit. The relative recovery of TIMP-1 was calculated as the ratio of TIMP-1 concentration in dialysate to its concentration in the medium surrounding the probe (11, 22). The relative recovery of TIMP-1 was 11.1 ± 0.3%. Recovery was constant between probes and within the probe for the TIMP-1 concentration range studied.

A fine-guiding needle (25 mm long, 0.51 mm OD, and 0.25 mm ID) was used for implantation of the dialysis probes. The guiding needle was connected to the dialysis probe with a stainless steel rod (5 mm long and 0.25 mm OD). Experimental protocols were initiated 2 h after implanting the dialysis probe. The dialysate sampling period was set at 60 min and was performed taking into account the dead space volume between the dialysis membrane and the sample tube.

Experimental protocol. After baseline dialysate was sampled and baseline hemodynamic data were recorded, the animals were randomized into the following three groups: *1*) VNS group ($n = 5$), in which electrical stimulation of vagal nerve was performed while the LV wall was perfused with Ringer solution via the dialysis probe; *2*) ACh group ($n = 8$), in which the LV wall was perfused with Ringer solution containing ACh (1 mM); and *3*) ACh-atropine (Atr) group ($n = 7$), in which the LV wall was perfused with Ringer solution containing ACh (1 mM) and Atr (0.2 mM). At 150 min after randomization, dialysate sampling and hemodynamic data recording were performed.

At the end of the experiment, the animal was euthanized. From selected hearts, transmural blocks of the LV free wall containing the dialysis probe were fixed in 4% paraformaldehyde for immunohistochemistry.

Immunohistochemistry and confocal microscopy. To investigate the distribution of TIMP-1, we performed confocal image analysis of LV tissue stained with anti-TIMP-1 antibody. Fixed blocks of LV tissues were washed in 0.1 mol/l phosphate buffer (pH 7.4), embedded in paraffin, and sectioned at a thickness of 5 μm. Sections were deparaffinized using xylene, rehydrated with serial grades of ethanol, and followed by hydration with distilled water. For antigen retrieval of TIMP-1 protein, specimens were immersed in a vessel filled with Target Retrieval Solution (pH 6.1; DAKO). The vessel containing the specimens was autoclaved at 121°C for 20 min. The slides were then allowed to cool at room temperature for 20 min to complete antigen unmasking. The sections were then incubated for 30 h with a mouse anti-TIMP-1 antibody (7-6C1, Daiichi Fine Chemical) diluted 1:5 and then incubated for 2 h in Alexa-488-conjugated goat anti-mouse Ig-G (Molecular Probes) diluted 1:200. Fluorescence of Alexa-488 was observed with a confocal laser-scanning microscope system (FV 300, Olympus). Reconstructed projection images were obtained from serial optical sections recorded at an interval of 0.5 μm.

Exclusion Criteria

Animals were excluded from the study when the following criteria were met: *1*) in the I/R study, coronary artery occlusion did not produce substantial regional dysfunction (FS of the risk area after occlusion was not <20% of the baseline value); *2*) intractable ventricular fibrillation or atrial tachycardia occurred; and *3*) the animal died during the surgical procedure, and the protocol was not completed.

Statistical Analysis

All data are presented as means ± SE. Tukey-Welsch's step-down multiple comparison test was used to determine the significance of differences among groups. P values <0.05 were considered statistically significant.

RESULTS

I/R Study

As shown in Fig. 1*A*, zymography of the myocardial extracts detected two bands at 92 and 72 kDa, corresponding to MMP-9 and MMP-2, respectively. Densitometric analysis demonstrated that relative MMP-9 level increased to a similar degree in the I/R and I/R-VS groups compared with the sham and VS groups (Fig. 1*B*). The relative MMP-2 level decreased in the I/R group compared with the sham and I/R-VS groups (Fig. 1*C*).

Bioactivity assays demonstrated that myocardial levels of total MMP-9 protein increased to a similar degree in the I/R and I/R-VS groups compared with sham and VS groups (Fig. 2*A*). Levels of endogenous active MMP-9 protein also increased in the I/R and I/R-VS groups compared with the sham and VS groups (Fig. 2*B*). The level of active MMP-9 in the I/R-VS group was significantly lower than that in the I/R group (<50%, $P < 0.01$).

The myocardial level of TIMP-1 protein increased in the VS and I/R-VS groups compared with the sham and I/R groups (Fig. 3*A*). There was no significant difference in the myocardial level of TIMP-2 protein among the four groups (Fig. 3*B*). TIMP-1 mRNA as measured by real-time RT-PCR was increased in the I/R-VS group compared with the sham, VS, and I/R groups (Fig. 3*C*).

Table 2 summarizes the data of systemic hemodynamics and LV function during the I/R study. In the VS and I/R-VS groups, HR decreased significantly compared with sham and I/R values at 60 and 240 min. In the I/R and I/R-VS groups, FS was depressed during ischemia with only partial recovery after reperfusion. In the I/R and I/R-VS groups, sonomicrometry demonstrated early systolic bulging of the anterior LV wall during ischemia as reflected by negative FS at the 60-min time point. There was no significant difference in LV dP/dt_{max} and FS between the I/R and I/R-VS groups at 60 and 240 min.

Cardiac Microdialysis Study

Figure 4 presents dialysate TIMP-1 concentrations in response to electrical stimulation of the vagal nerve, to perfusion of ACh, and to perfusion of ACh with Atr. There were no

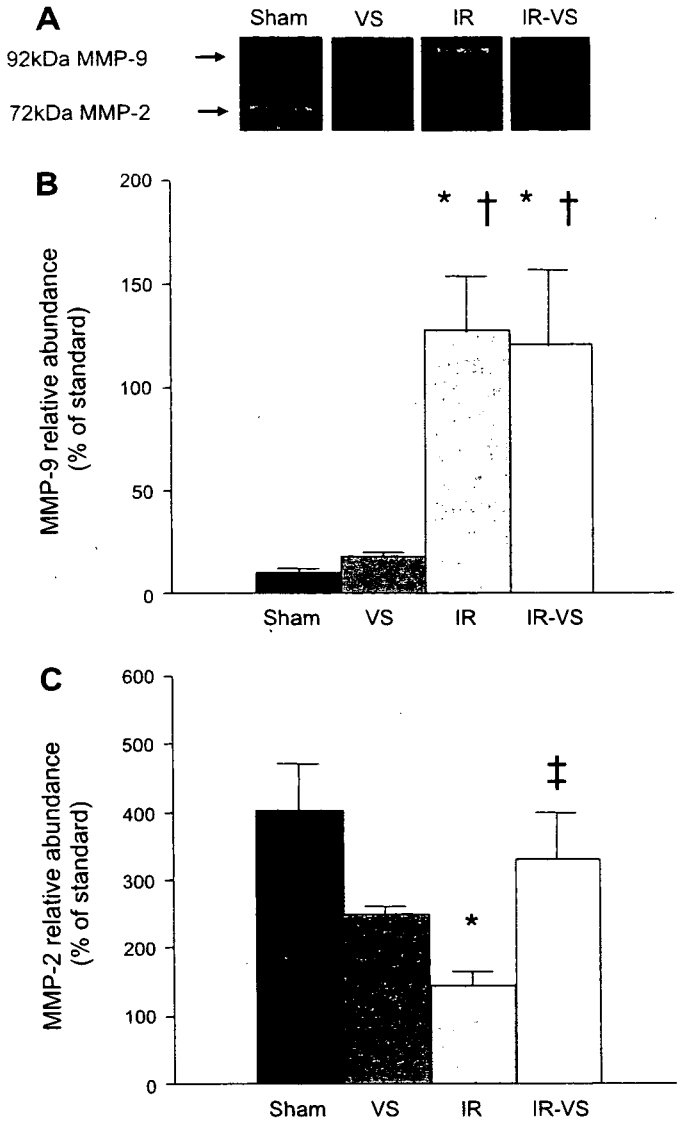

Fig. 1. Zymographic analysis of matrix metalloproteinase (MMP)-9 and -2 proteins in isolated myocardium. Sham, no myocardial ischemia and no vagal stimulation; VS, no myocardial ischemia with vagal stimulation; I/R, myocardial ischemia-reperfusion; I/R-VS, myocardial ischemia-reperfusion with VS. *A*: representative zymogram showing MMP-9 at 92 kDa and MMP-2 at 72 kDa. *B*: densitometric analysis of relative MMP-9 content expressed as percentage of standard. *C*: densitometric analysis of relative MMP-2 content expressed as percentage of standard. Data are means ± SE. $*P < 0.01$ vs. sham; $\dagger P < 0.01$ vs. VS; $\ddagger P < 0.05$ vs. I/R.

significant differences in baseline TIMP-1 concentrations among the three groups. At 150 min, dialysate TIMP-1 concentration was significantly higher in the VNS and ACh groups than in the ACh-Atr group ($P < 0.05$).

Figure 5 depicts representative microscopic findings of LV tissue around the microdialysis probes in the VNS, ACh, and ACh-Atr groups. Hematoxylin-eosin-stained sections demonstrated only a minimum hemorrhage around the dialysis probe (Fig. 5, *A–C*). TIMP-1-positive cardiomyocytes were detected sparsely but in diffuse distribution throughout the myocardium in the VNS group (Fig. 5*D*). TIMP-1-positive cardiomyocytes were detected over a relatively wide area around the dialysis probe in the ACh group (Fig. 5*E*). TIMP-1-positive cardiomyocytes were also detected but localized close to the dialysis probe in the ACh-Atr group (Fig. 5*F*). Immunoreactive signals of TIMP-1 were restricted to the cytoplasm of cardiomyocytes in all the groups (Fig. 5, *G–I*).

Table 3 summarizes the data of systemic hemodynamics and LV function during the cardiac microdialysis study. In the VNS group, HR decreased significantly compared with that in the ACh and ACh-Atr groups at 150 min. In the ACh and ACh-Atr groups, topical perfusion of ACh or ACh with Atr did not affect the systemic hemodynamics and the LV functions. Except for HR, there were no significant differences in other hemodynamic parameters among the three groups.

DISCUSSION

The major new findings of the present study were as follows. In ischemia-reperfused myocardium, stimulation of the efferent vagal nerve increased TIMP-1 mRNA and protein levels and reduced endogenous active MMP-9 protein. In normal myocardium, VNS or topical perfusion of ACh through a microdialysis probe increased dialysate TIMP-1 protein level. An increase in the dialysate TIMP-1 protein level induced by ACh perfusion was suppressed by coperfusion of Atr.

The robust increase in total MMP-9 levels after reperfusion in this study (Figs. 1*B* and 2*A*) might be mainly due to the

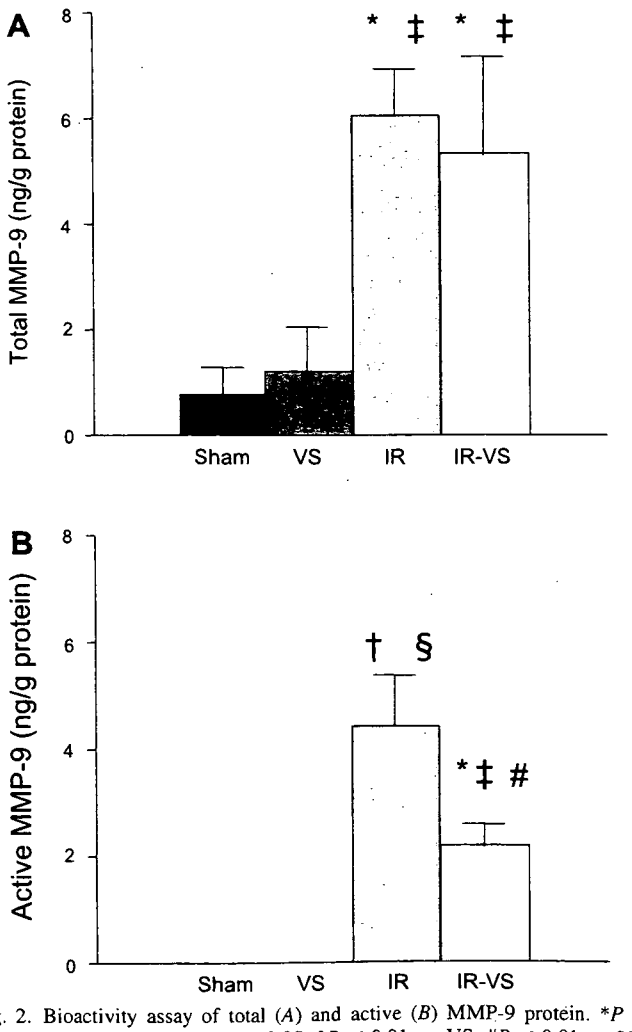

Fig. 2. Bioactivity assay of total (*A*) and active (*B*) MMP-9 protein. $*P < 0.05$; $\dagger P < 0.01$ vs. sham; $\ddagger P < 0.05$; $\S P < 0.01$ vs. VS. $\#P < 0.01$ vs. I/R.

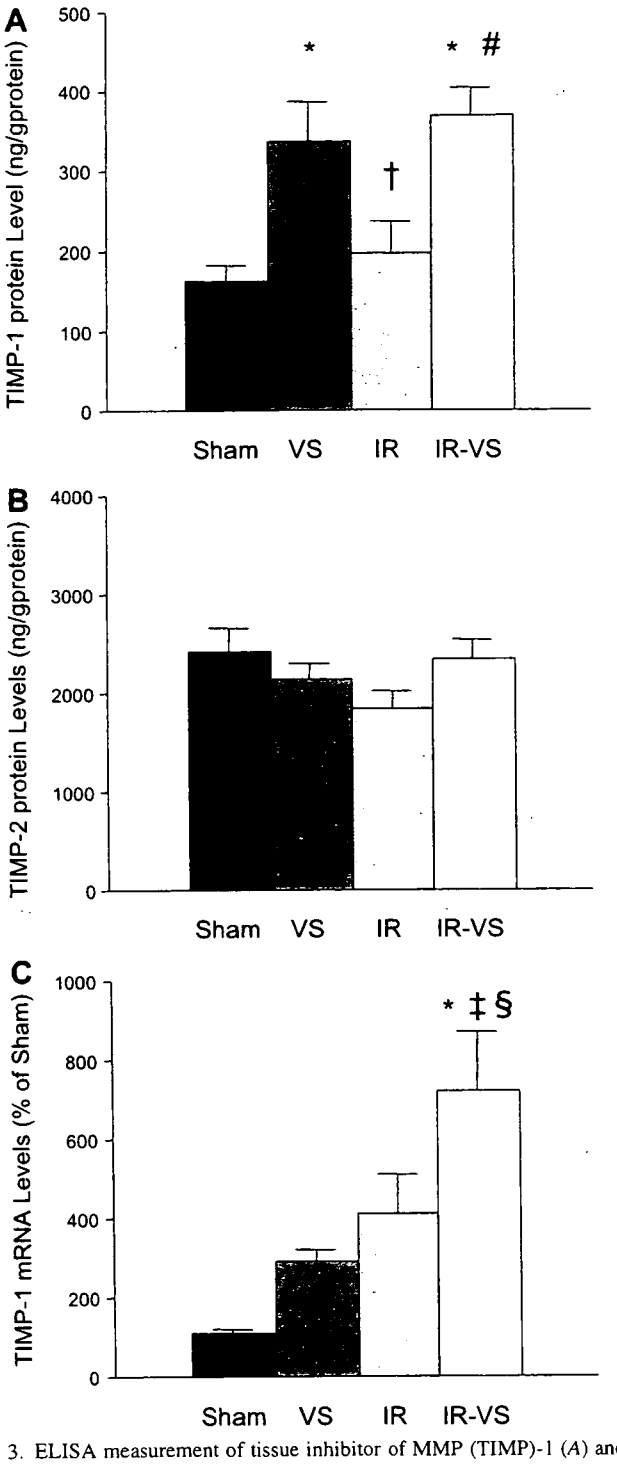

Fig. 3. ELISA measurement of tissue inhibitor of MMP (TIMP)-1 (*A*) and -2 (*B*) protein. Real-time RT-PCR analysis of TIMP-1 mRNA expressed as percentage of sham (*C*). *$P < 0.01$ vs. sham; †$P < 0.05$; ‡$P < 0.01$ vs. VS; §$P < 0.05$; #$P < 0.01$ vs. I/R.

infiltrated neutrophils. Although all cell types, including cardiomyocytes (25, 34) and endothelial cells (41), express MMP-9, neutrophil is an important source of MMP-9 after I/R (26). The level of endogenous active MMP-9 was lower in the I/R-VS group than in the I/R group (Fig. 2*B*). Increased expression of TIMP-1 by VNS (Fig. 3) likely inhibited the conversion of pro-MMP-9 to active MMP-9 and/or inhibited

Table 2. *Hemodynamic parameters during I/R study*

	Baseline	60 min	240 min
HR, beats/min			
Sham	317±9	334±7	326±9
VS	281±14	215±17*‡	238±19*‡
I/R	306±9	316±9	314±8
I/R-VS	301±7	217±5*‡	228±8*‡
MAP, mmHg			
Sham	92±3	93±4	92±3
VS	98±4	91±5	89±5
I/R	102±3	95±4	88±6
I/R-VS	99±4	88±4	83±2
LV dP/dt_{max}, mmHg/s			
Sham	5,119±263	5,308±388	4,819±339
VS	5,040±381	3,993±319	4,140±302
I/R	5,524±423	5,276±404	4,514±467
I/R-VS	5,672±360	4,549±250	4,079±188
FS, %			
Sham	10.8±0.9	10.1±1.0	9.3±1.0
VS	12.2±1.1	11.1±1.2	10.4±1.6
I/R	8.7±0.8	−0.6±0.6*†	0.1±0.8*†
I/R-VS	8.5±1.3	−0.6±0.4*†	1.5±0.7*†

Values are means ± SE. Sham group, no myocardial ischemia and no vagal stimulation (VS); VS group, no myocardial ischemia with VS; I/R group, myocardial ischemia-reperfusion (I/R); IR-VS, myocardial I/R with VS; HR, heart rate; MAP, mean arterial pressure; LV dP/dt_{max}, maximum first derivative of left ventricular (LV) pressure; FS, fractional shortening of anterior wall (risk area). *$P < 0.01$ vs. sham; †$P < 0.01$ vs. VS; ‡$P < 0.01$ vs. I/R.

activé MMP-9 itself more potently than in the case without VNS (14). Oxygen free radical induces expression and activation of MMP-9 (17, 41). Reduction of HR by VNS probably reduced myocardial oxygen consumption, ameliorated myocardial ischemia, and reduced oxygen free radicals (30). This may contribute to some extent to the reduction of active MMP-9 in the I/R-VS group.

In the I/R study, TIMP-1 mRNA was significantly higher in the I/R-VS group compared with the sham, VS, and I/R groups (Fig. 3*C*). TIMP-1 mRNA appeared higher in the VS and I/R groups compared with the sham group, although the differences were not significant. Stapel et al. (38) noted increased expression of TIMP-1 mRNA after myocardial I/R in mice. Proinflammatory cytokines such as interleukin-1β induced by

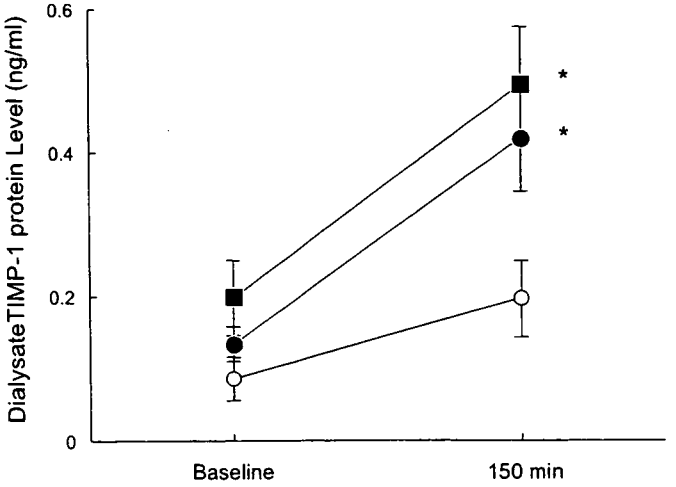

Fig. 4. Dialysate TIMP-1 protein concentration in response to vagal nerve stimulation (■), perfusion of acetylcholine (ACh; ●), or ACh with atropine (Atr) (○). *$P < 0.05$ vs. perfusion of ACh with Atr.

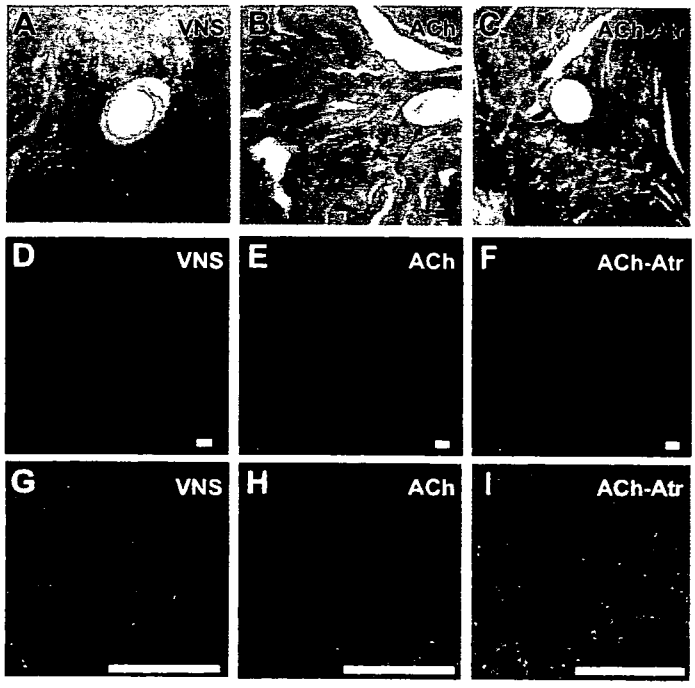

Fig. 5. Representative microscopic finding of left ventricular (LV) tissue implanted with microdialysis probe. *A–C*: hematoxylin and eosin-stained section of LV tissue perfused with Ringer solution under vagal nerve stimulation (VNS; *A*), perfused with ACh (*B*), and perfused with ACh and Atr (ACh-Atr; *C*). *D–F*: anti-TIMP-1 antibody (green)-immunostained sections of LV tissue perfused with Ringer solution under VNS (*D*), perfused with ACh (*E*), and perfused with ACh-Atr (*F*). *G–I*: higher magnifications of *D–F*, respectively. Arrows indicate dialysis probes. Bar = 100 μm.

myocardial ischemia are known to induce TIMP-1 (4). VNS and myocardial ischemia likely exerted an additive effect on the induction of TIMP-1 mRNA in the I/R-VS group. TIMP-1 protein levels in the VS and I/R-VS groups were significantly elevated compared with the sham and I/R groups (Fig. 3*A*). Figure 3, *A* and *C*, indicates dissociation between TIMP-1 mRNA and protein synthesis among the four groups. If the TIMP-1 protein level had correlated with the mRNA level, TIMP-1 protein level in the I/R and I/R-VS groups should have been higher than those presented in Fig. 3*A*. In myocardial ischemia, protein synthesis decreases owing to the inhibition of peptide chain elongation (8, 18). This may have partially inhibited TIMP-1 protein synthesis in the I/R and I/R-VS groups.

In the cardiac microdialysis study, the ACh-induced release of TIMP-1 was mediated by muscarinic ACh receptors because Atr blocked the increase in TIMP-1 in response to ACh stimulation (Fig. 4). TIMP-1 was produced by cardiomyocytes (Fig. 5, *G–I*). These findings suggest that VNS may induce TIMP-1 mRNA expression through muscarinic ACh receptors in cardiomyocytes and increase TIMP-1 protein content in myocardium. The distribution of TIMP-1-positive cardiomyocytes was different among the three groups (Fig. 5, *D–F*). This may reflect differences in the distribution of ACh among the three groups. ACh probably had a diffuse distribution in the myocardium in the VNS group but was concentrated around the dialysis probe in ACh group, whereas the effect of ACh concentrated around the dialysis probe was antagonized by Atr in the ACh-Atr group.

In addition to cardiomyocytes (25, 34), a variety of cell types, such as fibroblasts (14) and endothelial cells (6), produces and secretes TIMP-1. TIMP-1 expression in these cell types is low in the basal condition but is transcriptionally induced by various agents, including the cytokines, serum, growth factors, and phorbol esters (14). The signal transduction pathway from muscarinic ACh receptor stimulation to the induction of the TIMP-1 gene is not clear. Further elucidation of this is not in the scope of this study. ACh increases the production of nitric oxide from cardiomyocytes (9). Nitric oxide induces TIMP-1 gene expression by activating the transforming growth factor-β/Smad signaling pathway in glomerular mesangial cells in the kidney (2). These mechanisms may be involved in the increases in TIMP-1 mRNA and protein induced by VNS in myocardial I/R observed in the present study. Further studies are clearly required to elucidate these issues.

Myocardial expression of TIMP-2 was not modified by VNS (Fig. 3*B*). Contrary to the highly responsive nature of TIMP-1 expression to stimuli, TIMP-2 expression is, for the most part, constitutive (14). Previous studies demonstrated that ischemic injury or change in loading condition had little effect on myocardial expression of TIMP-2 (24, 25, 29). Myocardial content of MMP-2 decreased after I/R, and the decrease was inhibited by VNS (Fig. 1*C*). Cheung et al. (5) demonstrated that MMP-2 was released from the myocardium into the coronary effluent following myocardial I/R, resulting in the depletion of myocardial content of MMP-2.

In the present study, VNS did not prevent contractile dysfunction after I/R (Table 2). Actions of MMP and TIMP did not seem to be responsible for acute mechanical changes. Lu et al. (29) demonstrated that treatment with the MMP inhibitor failed to prevent acute myocardial dysfunction and regional expansion after I/R injury. The duration of reperfusion in our study (180 min) and that in Lu et al. (90 min) (29) may be too short to detect a significant influence of MMP and TIMP on regional LV function, which may become evident after a longer period of reperfusion.

Table 3. *Hemodynamic parameters during cardiac microdialysis study*

	Baseline	150 min
HR, beat/min		
VNS	286±7	227±7*†
ACh	303±16	308±9
ACh-Atr	304±14	298±16
MAP, mmHg		
VNS	101±8	103±8
ACh	93±3	100±4
ACh-Atr	87±3	92±6
LV dP/dr_{max}, mmHg/s		
VNS	5,050±588	4,768±475
ACh	5,203±345	5,488±400
ACh-Atr	4,519±269	4,718±450
FS, %		
VNS	7.4±1.8	7.2±1.9
ACh	5.0±1.2	4.9±1.2
ACh-Atr	5.4±0.5	5.0±0.5

Values are means ± SE. VNS group, LV tissue was perfused with Ringer solution via a dialysis probe under vagal nerve stimulation; ACh group, LV tissue was perfused with Ringer solution containing ACh (1 mM) via a dialysis probe; ACh-Atr group, LV tissue was perfused with ACh (1 mM) and atropine (0.2 mM) via a dialysis probe. *$P < 0.01$ vs. ACh; †$P < 0.01$ vs. ACh-Atr.

Several previous studies (10, 35, 39) demonstrated that targeted deletion of MMP-9 and/or the upregulation of TIMP-1 reduced infarct size, prevented LV rupture, and ameliorated LV remodeling after MI. Conversely, the expression of other MMPs, such as MMP-2, has been shown to be important in the myocardial healing that occurs in the later phases after ischemic injury (10). These observations suggest that the beneficial effect of VNS on LV remodeling after MI observed in our previous study (23) may be in a part mediated through the modified expression of MMPs and TIMPs as noted in the present study.

Except for the post-MI LV remodeling, MMPs and TIMPs contribute to the progression of various cardiovascular disorders, including expansion and rupture of aortic aneurysm (44), progression of acute viral myocarditis (15), and restenosis after coronary intervention (12). Local overexpression of TIMP-1 prevented the expansion and rupture of aortic aneurysm in rats (3) or prevented cardiac injury and dysfunction during experimental viral myocarditis in mice (15). VNS may be an effective biological inducer of TIMP-1 for the treatment of these disorders.

Limitation

The present study examined a limited number of MMP and TIMP species over a very short duration after myocardial I/R. A number of MMP and TIMP species are expressed in the myocardium, and several have been identified to be upregulated in cardiac disorders (24). Myocardial MMP-1 (collagenase) is induced by I/R (29). The actions of MMP-1 are inhibited in part by TIMP-1 (31). These suggest that VNS may inhibit the activity of MMP-1 in myocardial I/R injury. Further studies to define the effect of VNS on the profile of MMPs and TIMPs expressed in the myocardium are warranted.

In the present study, VNS was started 15 min before coronary occlusion. We did not examine whether VNS started after the coronary artery occlusion or whether reperfusion is capable of increasing myocardial TIMP-1. The pretreatment strategy as adopted in this study is unrealistic in clinical practice. Therefore, further studies are required to examine the time factor of VNS.

Concentration of ACh perfused through the dialysis probe in this study (1 mM) was substantially higher than the dialysate concentration of endogenous ACh released from the myocardium (<20 nM) (1). The ACh concentration within the myocardial interstitium might have been elevated over the supraphysiological range in the present microdialysis study. However, even if the interstitial concentration of ACh was unphysiologically high, Atr blocked the increase in TIMP-1 expression in response to ACh stimulation. Therefore, it is fair to say that TIMP-1 expression in response to ACh stimulation is mediated through the muscarinic ACh receptor.

TIMP-1 binds with MMPs to form a rather high molecular weight complex. Our preliminary in vitro experiment demonstrated that the relative recovery of TIMP-1/lipocalin/MMP-9 complex (Calbiochem, La Jolla, CA) was 3.8 ± 1.3% (range 0–5.5%) and was lower than that for free TIMP-1 (11.1 ± 0.3%) (see METHODS). Although the presence of MMPs, especially MMP-9, could affect the measurement of TIMP-1 within the myocardium by our microdialysis method, this probably does not affect the conclusion drawn from the cardiac microdialysis study, because the study was conducted in a heart free of I/R, which might contain low levels of myocardial MMP-9 as inferred from the results of the I/R study.

CONCLUSION

In a rabbit model of myocardial I/R injury, VNS induced TIMP-1 expression in cardiomyocytes and reduced active MMP-9.

GRANTS

This study was supported by a grant-in-aid for Scientific Research (C) (18500358) from the Ministry of Education, Culture, Sports, Science and Technology; by Health and Labour Sciences research grants for research on medical devices for analyzing, supporting and substituting the function of human body (H15-physi-001) from the Ministry of Health, Labour and Welfare of Japan; and by a research grant from the Fukuda Foundation for Medical Technology.

REFERENCES

1. **Akiyama T, Yamazaki T.** Adrenergic inhibition of endogenous acetylcholine release on postganglionic cardiac vagal nerve terminals. *Cardiovasc Res* 46: 531–538, 2000.
2. **Akool el-S, Doller A, Muller R, Gutwein P, Xin C, Huwiler A, Pfeilschifter J, Eberhardt W.** Nitric oxide induces TIMP-1 expression by activating the transforming growth factor beta-Smad signaling pathway. *J Biol Chem* 280: 39403–39416, 2005.
3. **Allaire E, Forough R, Clowes M, Starcher B, Clowes AW.** Local overexpression of TIMP-1 prevents aortic aneurysm degeneration and rupture in a rat model. *J Clin Invest* 102: 1413–1420, 1998.
4. **Chandrasekar B, Smith JB, Freeman GL.** Ischemia-reperfusion of rat myocardium activates nuclear factor-KappaB and induces neutrophil infiltration via lipopolysaccharide-induced CXC chemokine. *Circulation* 103: 2296–2302, 2001.
5. **Cheung PY, Sawicki G, Wozniak M, Wang W, Radomski MW, Schulz R.** Matrix metalloproteinase-2 contributes to ischemia-reperfusion injury in the heart. *Circulation* 101: 1833–1839, 2000.
6. **Chua CC, Hamdy RC, Chua BH.** Angiotensin II induces TIMP-1 production in rat heart endothelial cells. *Biochim Biophys Acta* 1311: 175–180, 1996.
7. **Chua PK, Melish ME, Yu Q, Yanagihara R, Yamamoto KS, Nerurkar VR.** Elevated levels of matrix metalloproteinase 9 and tissue inhibitor of metalloproteinase 1 during the acute phase of Kawasaki disease. *Clin Diagn Lab Immunol* 10: 308–314, 2003.
8. **Crozier SJ, Vary TC, Kimball SR, Jefferson LS.** Cellular energy status modulates translational control mechanisms in ischemic-reperfused rat hearts. *Am J Physiol Heart Circ Physiol* 289: H1242–H1250, 2005.
9. **Dedkova EN, Ji X, Wang YG, Blatter LA, Lipsius SL.** Signaling mechanisms that mediate nitric oxide production induced by acetylcholine exposure and withdrawal in cat atrial myocytes. *Circ Res* 93: 1233–1240, 2003.
10. **Ducharme A, Frantz S, Aikawa M, Rabkin E, Lindsey M, Rohde LE, Schoen FJ, Kelly RA, Werb Z, Libby P, Lee RT.** Targeted deletion of matrix metalloproteinase-9 attenuates left ventricular enlargement and collagen accumulation after experimental myocardial infarction. *J Clin Invest* 106: 55–62, 2000.
11. **Ergul A, Walker CA, Goldberg A, Baicu SC, Hendrick JW, King MK, Spinale FG.** ET-1 in the myocardial interstitium: relation to myocyte ECE activity and expression. *Am J Physiol Heart Circ Physiol* 278: H2050–H2056, 2000.
12. **Feldman LJ, Mazighi M, Scheuble A, Deux JF, De Benedetti E, Badier-Commander C, Brambilla E, Henin D, Steg PG, Jacob MP.** Differential expression of matrix metalloproteinases after stent implantation and balloon angioplasty in the hypercholesterolemic rabbit. *Circulation* 103: 3117–3122, 2001.
13. **Fujimoto N, Zhang J, Iwata K, Shinya T, Okada Y, Hayakawa T.** A one-step sandwich enzyme immunoassay for tissue inhibitor of metalloproteinases-2 using monoclonal antibodies. *Clin Chim Acta* 220: 31–45, 1993.
14. **Gomez DE, Alonso DF, Yoshiji H, Thorgeirsson UP.** Tissue inhibitors of metalloproteinases: structure, regulation and biological functions. *Eur J Cell Biol* 74: 111–122, 1997.

15. **Heymans S, Pauschinger M, De Palma A, Kallwellis-Opara A, Rutschow S, Swinnen M, Vanhoutte D, Gao F, Torpai R, Baker AH, Padalko E, Neyts J, Schultheiss HP, Van de Werf F, Carmeliet P, Pinto YM.** Inhibition of urokinase-type plasminogen activator or matrix metalloproteinases prevents cardiac injury and dysfunction during viral myocarditis. *Circulation* 114: 565–573, 2006.
16. **Hudson MP, Armstrong PW, Ruzyllo W, Brum J, Cusmano L, Krzeski P, Lyon R, Quinones M, Theroux P, Sydlowski D, Kim HE, Garcia MJ, Jaber WA, Weaver WD.** Effects of selective matrix metalloproteinase inhibitor (PG-116800) to prevent ventricular remodeling after myocardial infarction: results of the PREMIER (Prevention of Myocardial Infarction Early Remodeling) trial. *J Am Coll Cardiol* 48: 15–20, 2006.
17. **Kameda K, Matsunaga T, Abe N, Hanada H, Ishizaka H, Ono H, Saitoh M, Fukui K, Fukuda I, Osanai T, Okumura K.** Correlation of oxidative stress with activity of matrix metalloproteinase in patients with coronary artery disease. Possible role for left ventricular remodelling. *Eur Heart J* 24: 2180–2185, 2003.
18. **Kao R, Rannels DE, Morgan HE.** Effects of anoxia and ischemia on protein synthesis in perfused rat hearts. *Circ Res* 38, *Suppl* 1: I124–I130, 1976.
19. **Kitagawa H, Yamazaki T, Akiyama T, Sugimachi M, Sunagawa K, Mori H.** Microdialysis separately monitors myocardial interstitial myoglobin during ischemia and reperfusion. *Am J Physiol Heart Circ Physiol* 289: H924–H930, 2005.
20. **Kodama S, Iwata K, Iwata H, Yamashita K, Hayakawa T.** Rapid one-step sandwich enzyme immunoassay for tissue inhibitor of metalloproteinases. An application for rheumatoid arthritis serum and plasma. *J Immunol Methods* 127: 103–108, 1990.
21. **La Rovere MT, Bigger JT Jr, Marcus FI, Mortara A, Schwartz PJ.** Baroreflex sensitivity and heart-rate variability in prediction of total cardiac mortality after myocardial infarction. ATRAMI (Autonomic Tone and Reflexes After Myocardial Infarction) Investigators. *Lancet* 351: 478–484, 1998.
22. **Le Quellec A, Dupin S, Genissel P, Saivin S, Marchand B, Houin G.** Microdialysis probes calibration: gradient and tissue dependent changes in no net flux and reverse dialysis methods. *J Pharmacol Toxicol Methods* 33: 11–16, 1995.
23. **Li M, Zheng C, Sato T, Kawada T, Sugimachi M, Sunagawa K.** Vagal nerve stimulation markedly improves long-term survival after chronic heart failure in rats. *Circulation* 109: 120–124, 2004.
24. **Li YY, Feldman AM, Sun Y, McTiernan CF.** Differential expression of tissue inhibitors of metalloproteinases in the failing human heart. *Circulation* 98: 1728–1734, 1998.
25. **Li YY, Feng Y, McTiernan CF, Pei W, Moravec CS, Wang P, Rosenblum W, Kormos RL, Feldman AM.** Downregulation of matrix metalloproteinases and reduction in collagen damage in the failing human heart after support with left ventricular assist devices. *Circulation* 104: 1147–1152, 2001.
26. **Lindsey M, Wedin K, Brown MD, Keller C, Evans AJ, Smolen J, Burns AR, Rossen RD, Michael L, Entman M.** Matrix-dependent mechanism of neutrophil-mediated release and activation of matrix metalloproteinase 9 in myocardial ischemia/reperfusion. *Circulation* 103: 2181–2187, 2001.
27. **Lindsey ML, Gannon J, Aikawa M, Schoen FJ, Rabkin E, Lopresti-Morrow L, Crawford J, Black S, Libby P, Mitchell PG, Lee RT.** Selective matrix metalloproteinase inhibition reduces left ventricular remodeling but does not inhibit angiogenesis after myocardial infarction. *Circulation* 105: 753–758, 2002.
28. **Livak KJ, Schmittgen TD.** Analysis of relative expression data using real-time quantitative PCR and the $2^{-\Delta\Delta C_t}$ method. *Methods* 25: 402–408, 2001.
29. **Lu L, Gunja-Smith Z, Woessner JF, Ursell PC, Nissen T, Galardy RE, Xu Y, Zhu P, Schwartz GG.** Matrix metalloproteinases and collagen ultrastructure in moderate myocardial ischemia and reperfusion in vivo. *Am J Physiol Heart Circ Physiol* 279: H601–H609, 2000.
30. **Mioni C, Bazzani C, Giuliani D, Altavilla D, Leone S, Ferrari A, Minutoli L, Bitto A, Marini H, Zaffe D, Botticelli AR, Iannone A, Tomasi A, Bigiani A, Bertolini A, Squadrito F, Guarini S.** Activation of an efferent cholinergic pathway produces strong protection against myocardial ischemia/reperfusion injury in rats. *Crit Care Med* 33: 2621–2628, 2005.
31. **Moe SM, Singh GK, Bailey AM.** Beta2-microglobulin induces MMP-1 but not TIMP-1 expression in human synovial fibroblasts. *Kidney Int* 57: 2023–2034, 2000.
32. **Mukherjee R, Brinsa TA, Dowdy KB, Scott AA, Baskin JM, Deschamps AM, Lowry AS, Escobar GP, Lucas DG, Yarbrough WM, Zile MR, Spinale FG.** Myocardial infarct expansion and matrix metalloproteinase inhibition. *Circulation* 107: 618–625, 2003.
33. **Pfeffer MA, Braunwald E.** Ventricular remodeling after myocardial infarction. Experimental observations and clinical implications. *Circulation* 81: 1161–1172, 1990.
34. **Romanic AM, Burns-Kurtis CL, Gout B, Berrebi-Bertrand I, Ohlstein EH.** Matrix metalloproteinase expression in cardiac myocytes following myocardial infarction in the rabbit. *Life Sci* 68: 799–814, 2001.
35. **Romanic AM, Harrison SM, Bao W, Burns-Kurtis CL, Pickering S, Gu J, Grau E, Mao J, Sathe GM, Ohlstein EH, Yue TL.** Myocardial protection from ischemia/reperfusion injury by targeted deletion of matrix metalloproteinase-9. *Cardiovasc Res* 54: 549–558, 2002.
36. **Silvestry SC, Taylor DA, Lilly RE, Atkins BZ, Marathe US, Davis JW, Kraus W, Glower DD.** The in vivo quantification of myocardial performance in rabbits: a model for evaluation of cardiac gene therapy. *J Mol Cell Cardiol* 28: 815–823, 1996.
37. **Squire IB, Evans J, Ng LL, Loftus IM, Thompson MM.** Plasma MMP-9 and MMP-2 following acute myocardial infarction in man: correlation with echocardiographic and neurohumoral parameters of left ventricular dysfunction. *J Card Fail* 10: 328–333, 2004.
38. **Stapel H, Kim SC, Osterkamp S, Knuefermann P, Hoeft A, Meyer R, Grohe C, Baumgarten G.** Toll-like receptor 4 modulates myocardial ischaemia-reperfusion injury: role of matrix metalloproteinases. *Eur J Heart Fail* 8: 665–672, 2006.
39. **Trescher K, Bernecker O, Fellner B, Gyongyosi M, Schafer R, Aharinejad S, DeMartin R, Wolner E, Podesser BK.** Inflammation and postinfarct remodeling: overexpression of IkappaB prevents ventricular dilation via increasing TIMP levels. *Cardiovasc Res* 69: 746–754, 2006.
40. **Udelson JE, Konstam MA.** Relation between left ventricular remodeling and clinical outcomes in heart failure patients with left ventricular systolic dysfunction. *J Card Fail* 8: S465–S471, 2002.
41. **Uemura S, Matsushita H, Li W, Glassford AJ, Asagami T, Lee KH, Harrison DG, Tsao PS.** Diabetes mellitus enhances vascular matrix metalloproteinase activity: role of oxidative stress. *Circ Res* 88: 1291–1298, 2001.
42. **Verheijen JH, Nieuwenbroek NM, Beekman B, Hanemaaijer R, Verspaget HW, Ronday HK, Bakker AH.** Modified proenzymes as artificial substrates for proteolytic enzymes: colorimetric assay of bacterial collagenase and matrix metalloproteinase activity using modified prourokinase. *Biochem J* 323: 603–609, 1997.
43. **Webb CS, Bonnema DD, Ahmed SH, Leonardi AH, McClure CD, Clark LL, Stroud RE, Corn WC, Finklea L, Zile MR, Spinale FG.** Specific temporal profile of matrix metalloproteinase release occurs in patients after myocardial infarction: relation to left ventricular remodeling. *Circulation* 114: 1020–1027, 2006.
44. **Wilson WR, Anderton M, Schwalbe EC, Jones JL, Furness PN, Bell PR, Thompson MM.** Matrix metalloproteinase-8 and -9 are increased at the site of abdominal aortic aneurysm rupture. *Circulation* 113: 438–445, 2006.
45. **Winer J, Jung CK, Shackel I, Williams PM.** Development and validation of real-time quantitative reverse transcriptase-polymerase chain reaction for monitoring gene expression in cardiac myocytes in vitro. *Anal Biochem* 270: 41–49, 1999.

ELSEVIER

Autonomic Neuroscience: Basic and Clinical 137 (2007) 44–50

AUTONOMIC NEUROSCIENCE: Basic & Clinical

www.elsevier.com/locate/autneu

Regional difference in ischaemia-induced myocardial interstitial noradrenaline and acetylcholine releases

Toru Kawada [a,*], Toji Yamazaki [b], Tsuyoshi Akiyama [b], Toshiaki Shishido [a], Shuji Shimizu [a], Masaki Mizuno [a], Hidezo Mori [b], Masaru Sugimachi [a]

[a] *Department of Cardiovascular Dynamics, Advanced Medical Engineering Center, National Cardiovascular Center Research Institute, 5-7-1 Fujishirodai, Suita, Osaka 565-8565, Japan*

[b] *Department of Cardiac Physiology, National Cardiovascular Center Research Institute, Japan*

Received 18 May 2007; received in revised form 28 June 2007

Abstract

Knowledge of the regional differences in myocardial interstitial noradrenaline (NA) and acetylcholine (ACh) levels during ischaemia would be important to understand the abnormality of neuronal environment surrounding the ischaemic heart. Using a cardiac microdialysis technique, we compared ischaemia-induced changes in the myocardial interstitial NA and ACh levels among three groups of anesthetized cats: the anterior free wall of the left ventricle (ANT group, $n=7$; the left anterior descending coronary artery was occluded), the posterior free wall of the left ventricle (POST group, $n=6$; the left circumflex coronary artery was occluded), and the right ventricle (RV group, $n=6$; the right coronary artery was occluded). The maximum NA level was not different between the ANT and POST groups but was significantly lower in the RV group ($P<0.01$) [70 nM (SD 37), 106 nM (SD 99), and 7 nM (SD 10), respectively]. The maximum ACh level was not different between the ANT and POST groups but was significantly lower in the RV group ($P<0.05$) [16 nM (SD 7), 20 nM (SD 15), and 6 nM (SD 2), respectively]. In contrast, there were no significant differences in NA or ACh release in response to a local administration of ouabain (10 mM) among the ANT, POST, and RV groups ($n=6$ each). In conclusion, the regional difference of the ischaemic effects, rather than the regional difference in the functional distributions of sympathetic and vagal efferent nerve terminals, might contribute to the lower levels of ischaemia-induced NA and ACh releases in the RV group.

Keywords: Cardiac microdialysis; Coronary artery occlusion; Ouabain; Cats

The heart is under an incessant control by the autonomic nervous system. The principal molecule that affects the myocardium is noradrenaline (NA) for the sympathetic nerve and acetylcholine (ACh) for the parasympathetic nerve. Acute myocardial ischaemia causes abnormality of the neural regulation via mechanisms such as pathological cardio-cardiac reflexes and disruption of the nerves traversing the ischaemic region (Zipes 1990; Hainsworth, 1991; Elvan and Zipes, 1998; Armour, 1999; Kawada et al., 2002). Although occlusion of the left anterior descending coronary artery (LAD) has been shown to increase myocardial interstitial NA and ACh levels in the ischaemic region (Shindo et al., 1996; Kawada et al., 2000; Lameris et al., 2000), whether the effects of ischaemia on the myocardial interstitial NA and ACh levels are homogeneous within the left ventricle and between the left and right ventricles remains unknown. The cardio-depressor reflex similar to that induced by veratridine (the Bezold–Jarisch reflex) is frequently observed in inferoposterior but not in anterior myocardial infarction, suggesting the regional difference in the vagal afferent fibre distribution within the left ventricle (Thames et al., 1978; Walker et al., 1978). Regional differences are also reported in the distributions of sympathetic and vagal efferent nerves within the left ventricle and between the left and right ventricles

* Corresponding author. Tel.: +81 6 6833 5012x2427; fax: +81 6 6835 5403.

E-mail address: torukawa@res.ncvc.go.jp (T. Kawada).

1566-0702/$ - see front matter © 2007 Elsevier B.V. All rights reserved.
doi:10.1016/j.autneu.2007.07.001

(Pierpont et al., 1984; Schmid et al., 1978). We hypothesized that the effects of ischaemia on the myocardial interstitial NA and ACh levels would also show regional differences.

We used a cardiac microdialysis technique and measured dialysate NA and ACh concentrations as indices of myocardial interstitial NA and ACh levels in anesthetized cats (Akiyama et al., 1991, 1994; Yamazaki et al., 1997; Kawada et al., 2001). We compared ischaemia-induced changes in the myocardial interstitial NA and ACh levels among the following regions: the anterior free wall of the left ventricle (ANT group) perfused by the LAD, the posterior free wall of the left ventricle (POST group) perfused by the left circumflex coronary artery (LCX), and the right ventricle (RV group) perfused by the right coronary artery (RCA). In addition, we compared changes in the myocardial interstitial NA and ACh levels in response to a local administration of ouabain through the dialysis probe (Yamazaki et al., 1999; Kawada et al., 2001). The advantage of the local administration of ouabain might be that we can assess the transmitter releasing function of the sympathetic and vagal efferent nerve terminals in the working heart without significant effects on the systemic haemodynamics.

1. Materials and methods

1.1. Surgical preparation

Animal care was conducted in accordance with the *Guiding Principles for the Care and Use of Animals in the Field of Physiological Sciences* approved by the Physiological Society of Japan. All protocols were approved by the Animal Subjects Committee of the National Cardiovascular Center. Adult cats weighing 2.2 to 5.0 kg were anaesthetized via an intraperitoneal injection of pentobarbital sodium (30–35 mg/kg) and ventilated mechanically with room air mixed with oxygen. The depth of anaesthesia was maintained with a continuous intravenous infusion of pentobarbital sodium ($1–2$ mg kg^{-1} h^{-1}) through a catheter inserted into the right femoral vein. Mean systemic arterial pressure was measured from a catheter inserted into the right femoral artery. The heart rate was determined using an electrocardiogram.

We performed an ischaemia protocol and a local ouabain protocol in different animals. In each protocol, the experimental animals were divided into ANT, POST, and RV groups. In the ANT and POST groups, the left fifth and/or sixth ribs were resected to allow access to the heart. In the ANT group, a 3-0 silk suture was passed around the LAD just distal to the first diagonal branch for later occlusion. Using a fine guiding needle, a dialysis probe was implanted transversely into the anterior free wall of the left ventricle perfused by the LAD. In the POST group, a 3-0 silk suture was passed around the LCX for later occlusion, and a dialysis probe was implanted transversely into the posterior free wall of the left ventricle perfused by the LCX. In the RV group, the right fifth and/or sixth ribs were resected to expose the heart. A 3-0 silk suture was passed around the RCA for later occlusion. The right ventricular wall was picked up with a pair of forceps, and a dialysis probe was threaded transversely through the myocardium using a fine guiding needle. Heparin sodium (100 U/kg) was administered intravenously to prevent blood coagulation. A postmortem examination confirmed that the dialysis probe did not penetrate into the ventricular cavity. In the local ouabain protocol, similar experimental settings without a coronary snare were prepared for the three groups of animals.

1.2. Dialysis technique

The materials and properties of the dialysis probe have been described previously (Akiyama et al., 1991, 1994). Briefly, a dialysis fibre (13 mm length, 310 μm O.D., 200 μm I.D.; PAN-1200, 50,000 molecular weight cutoff, Asahi Chemical, Osaka, Japan) was glued at both ends to polyethylene tubes (25 cm length, 500 μm O.D., 200 μm I.D.). The dialysis probe was perfused at a rate of 2 μl/min with Ringer solution containing a cholinesterase inhibitor eserine (10^{-4} M). Two hours elapsed before the dialysate sampling was started to allow dialysate NA and ACh concentrations reached steady states. One sampling period was set at 15 min, which yielded a sample volume of 30 μl. The actual dialysate sampling lagged by 5 min behind a given collection period taking into account the dead space volume between the dialysis membrane and the sample tube. Each sample was collected in a microtube containing 3 μl of phosphate buffer

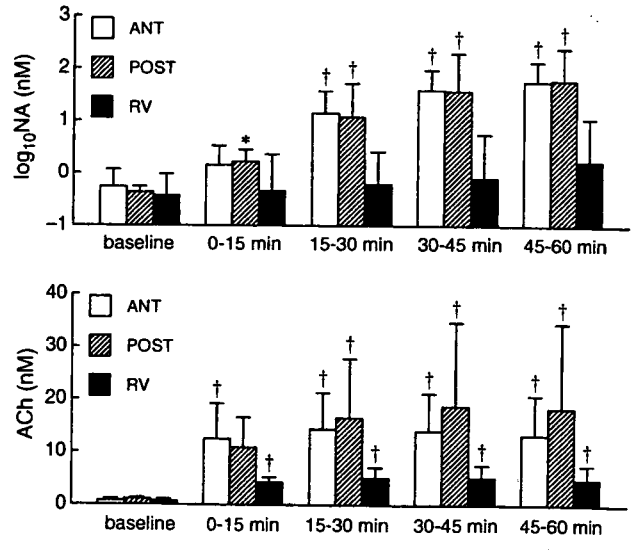

Fig. 1. Changes in myocardial interstitial noradrenaline (NA) and acetylcholine (ACh) levels during coronary occlusion. ANT: region of the anterior free wall of the left ventricle perfused by the left anterior descending coronary artery, POST: region of the posterior free wall of the left ventricle perfused by the left circumflex coronary artery, RV: region of the right ventricle perfused by the right coronary artery. The coronary occlusion significantly increased myocardial interstitial NA levels in the ANT and POST groups (top panel). Changes in the NA levels were not statistically significant in the RV group. The coronary occlusion significantly increased myocardial interstitial ACh levels in all of the ANT, POST, and RV groups (bottom panel). Data are mean and SD values. $^{*}P<0.05$ and $^{\dagger}P<0.01$ from the corresponding baseline value by Dunnett's test.

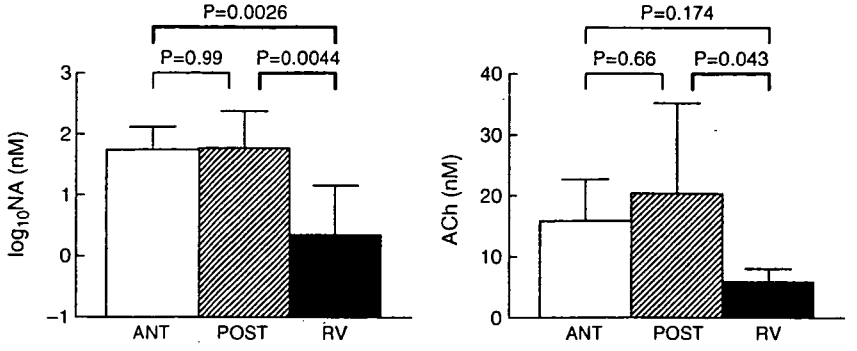

Fig. 2. Maximum levels of myocardial interstitial NA and ACh induced by coronary occlusions. The maximum NA level did not differ between the ANT and POST groups, but it was significantly lower in the RV group (left panel). The maximum ACh level did not differ between the ANT and POST groups, but it was significantly lower in the RV group than in the POST group (right panel). Data are mean and SD values. Exact P values determined by Tukey test are supplied.

(0.1 M, pH 3.5) to prevent amine oxidation. The ACh concentration in the dialysate was measured directly by high performance liquid chromatography with electrochemical detection (HPLC-ECD) system (Eicom, Kyoto, Japan). The NA concentration in the dialysate was measured by another HPLC-ECD system after removing interfering compounds with an alumina procedure.

1.3. Protocols

1.3.1. Ischaemia protocol

In each animal in the ANT ($n=7$), POST ($n=6$), and RV ($n=6$) groups, a 15-min dialysate sample was collected under baseline conditions. Thereafter, each corresponding coronary artery was occluded for 60 min, and four consecutive 15-min dialysate samples were obtained during the occlusion period.

1.3.2. Local ouabain protocol

In each animal in the ANT ($n=6$), POST ($n=6$), and RV ($n=6$) groups, a 15-min dialysate sample was collected under baseline conditions. The perfusate for the dialysis probe was then replaced with Ringer solution containing 10 mM of ouabain. The local administration of ouabain has been shown to evoke myocardial interstitial NA and ACh releases without significant effects on the systemic haemodynamics (Yamazaki et al., 1999; Kawada et al., 2001). Four consecutive 15-min dialysate samples were obtained during the local administration of ouabain.

1.4. Statistical analysis

All data are presented as mean (SD) values. Because the increase in NA reached more than 100 times the baseline value in the ANT and POST groups, NA data were compared after logarithmic transformation. To examine the effects of ischaemia or the local administration of ouabain on the NA or ACh level in each group, we used one-way repeated-measures analysis of variance (Glantz, 2002). When there was a significant difference in measured values among the collection periods, Dunnett's test was applied to identify the difference from the baseline value. To compare the maximum NA or ACh response among the ANT, POST, and RV groups, we used one-way analysis of variance. When there was a significant difference among the three groups, Tukey test was applied for simultaneous all pairwise comparisons. The differences were considered significant at $P<0.05$.

2. Results

Coronary artery occlusion increased the NA levels to more than 100 times the respective baseline levels in the ANT and POST groups (Fig. 1, top). In the RV group, although the mean NA level increased to nearly 10 times the baseline level, the change was not statistically significant, possibly due to the large variance of the NA responses across the animals. The coronary occlusion increased the ACh levels to approximately 15 times the respective baseline levels in the ANT and POST groups whereas it increased the

Table 1
Changes in mean arterial pressure by occlusions of the anterior descending coronary artery (ANT), the left circumflex coronary artery (POST), and the right coronary artery (RV)

	Baseline	5	15	30	45	60
ANT	116 (31)	114 (27)	108 (24)	108 (25)	108 (23)	110 (25)
POST	139 (31)	119 (31)†	125 (31)†	130 (31)*	132 (28)	135 (33)
RV	101 (20)	101 (26)	99 (22)	101 (23)	103 (25)	103 (23)

Baseline and values after 5, 15, 30, 45, and 60 min of the occlusion are presented (in mm Hg). Data are mean (SD) values. *$P<0.05$ and †$P<0.01$ from the corresponding baseline value.

Table 2
Changes in the heart rate by occlusions of the anterior descending coronary artery (ANT), the left circumflex coronary artery (POST), and the right coronary artery (RV)

	Baseline	5	15	30	45	60
ANT	193 (18)	166 (13)†	174 (15)†	175 (18)†	173 (15)†	171 (15)†
POST	183 (25)	159 (21)†	167 (20)†	167 (25)†	170 (25)†	169 (27)†
RV	188 (34)	175 (35)	176 (33)	179 (35)	181 (36)	183 (38)

Baseline and values after 5, 15, 30, 45, and 60 min of the occlusion are presented (in beats min^{-1}). Data are mean (SD) values. †$P<0.01$ from the corresponding baseline value.

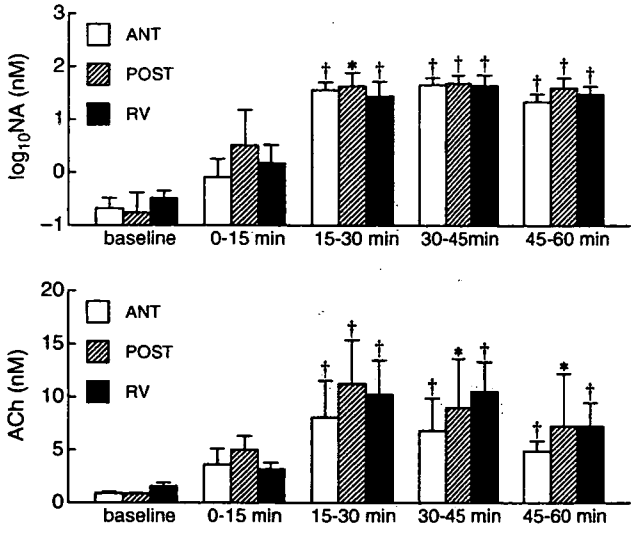

Fig. 3. Changes in myocardial interstitial NA and ACh levels induced by a local administration of ouabain through the dialysis probe. Ouabain significantly increased myocardial interstitial NA levels in all of the ANT, POST, and RV groups (top panel). The maximum NA level did not differ among the three groups. Ouabain significantly increased myocardial interstitial ACh levels in all of the ANT, POST, and RV groups (bottom panel). The maximum ACh level did not differ among the three groups. Data are mean and SD values. $^{*}P<0.05$ and $^{\dagger}P<0.01$ from the corresponding baseline value by Dunnett's test.

ACh levels to approximately 8 times the baseline level in the RV group (Fig. 1, bottom).

The maximum NA level observed during ischaemia was not different between the ANT and POST groups, but it was significantly lower in the RV group than in the ANT and POST groups (Fig. 2, left). The maximum ACh level observed during ischaemia was not different between the ANT and POST groups, but it was significantly lower in the RV group than in the POST group (Fig. 2, right).

Changes in mean arterial pressure obtained from the ischaemia protocol are summarized in Table 1. Occlusion of the LAD did not change mean arterial pressure significantly (the ANT group), whereas occlusion of the LCX significantly decreased mean arterial pressure at 5, 15, and 30 min of the ischaemic period (the POST group). Occlusion of the RCA did not change mean arterial pressure (the RV group).

Changes in the heart rate obtained from the ischaemia protocol are summarized in Table 2. Occlusion of the LAD significantly decreased the heart rate throughout the occlusion period (the ANT group). Occlusion of the LCX also significantly decreased the heart rate throughout the occlusion period (the POST group). In contrast, occlusion of the RCA did not change the heart rate significantly (the RV group).

A local administration of ouabain increased the NA levels in all of the ANT, POST, and RV groups (Fig. 3, top). There were no significant differences in the maximum NA levels among the three groups ($P=0.40$ by ANOVA). The local administration of ouabain also increased the ACh levels in all of the ANT, POST, and RV groups (Fig. 3, bottom). The ACh levels reached their maximum levels during 15–30 min of the administration period, then slightly decreased from the maximum levels during 30–45 and 45–60 min of the administration period but remained higher than the respective baseline levels. There were no significant differences in the maximum ACh levels among the three groups ($P=0.35$ by ANOVA).

3. Discussion

The level of ischaemia-induced NA release was significantly lower in the RV group than in the ANT and POST groups (Fig. 2, left). The level of ischaemia-induced ACh release was significantly lower in the RV group than in the POST group (Fig. 2, right). To our knowledge, this is the first report showing the differential effects of ischaemia on the myocardial interstitial NA and ACh levels among the main coronary arteries.

3.1. Regional difference in the ischaemia-induced myocardial interstitial NA release

Mechanisms responsible for the ischaemia-induced NA release have been extensively studied (Schömig A et al., 1984, 1988). An exocytotic release mechanism participates in the NA release in the early phase of ischaemia (within approximately 20 min from the onset of ischaemia) (Akiyama and Yamazaki, 1999). Energy depletion in the ischaemic region impairs the Na^+–K^+ ATPase activity and induces axoplasmic Na^+ accumulation. Because the NA uptake carrier is driven by the Na^+ gradient across the plasma membrane (Schwartz, 2000), the accumulation of intracellular Na^+ causes the reverse transport of axoplasmic NA to extracellular space. This nonexocytotic release mechanism becomes predominant as the ischaemic period is prolonged (Akiyama and Yamazaki, 1999; Lameris et al., 2000). In the present study, there was no significant difference in the levels of ischaemia-induced NA release between the ANT and POST groups (Fig. 2, left), suggesting that the extent of energy depletion caused by the coronary artery occlusion might be similar between the anterior and posterior regions of the left ventricle. In contrast, the level of ischaemia-induced NA release was much lower in the RV group (Fig. 2, left). Much lower oxygen consumption in the right ventricle than in the left ventricle (Weiss et al., 1978; Kusachi et al. 1982) may have delayed the progression of ischaemia and/or mitigated the severity of ischaemia.

To examine whether the observed difference in the ischaemia-induced NA release was attributable to the regional difference in the functional distribution of sympathetic efferent nerve terminals, we measured the amount of myocardial interstitial NA release in response to a local administration of ouabain (Yamazaki et al., 1999). Because locally administered ouabain spreads in the vicinity of the semipermeable membrane of the dialysis fibre and evokes the NA release, the NA concentration in the dialysate thus measured is considered to reflect the density of sympathetic

nerve terminals around the dialysis fibre. There were no significant differences in the maximum NA levels in response to the ouabain administration among the ANT, POST, and RV groups (Fig. 3, top), suggesting that the functional distribution of sympathetic efferent nerve terminals did not account for the lower level of ischaemia-induced NA release in the RV group.

The results of local administration of ouabain, showing no significant regional differences in the functional distribution of sympathetic efferent nerve terminals, are comparable to histological studies. In the human heart (Kawano et al., 2003), the number of tyrosine hydroxylase (TH)-positive nerves is similar between the left and right ventricles, and the number of TH-positive nerves in the anterior wall is 1.2 times greater than that in the posterior wall of the left ventricle. Although Pierpont et al. (Pierpont et al., 1984) reported a regional difference in the NA content in the canine left ventricle, the major difference observed in their study is an increasing gradient of NA from the apex to the base of the ventricle. In addition, the NA content was similar between the left and right ventricles in their study [495 ng/g (SD 267) vs. 503 ng/g (SD 123)].

3.2. Regional difference in the ischaemia-induced myocardial interstitial ACh release

In previous studies, we have demonstrated that acute myocardial ischaemia causes myocardial interstitial ACh release in the ischaemic region (Kawada et al., 2000; 2006b). An exocytotic release mechanism may be involved in the ischaemia-induced ACh release within approximately 15 min from the onset of ischaemia (Kawada et al., 2000, 2006a). Thereafter, a local ACh release mechanism independent of vagal nerve discharge may play a dominant role in the ischaemia-induced ACh release. In the present study, there was no significant difference in the levels of ischaemia-induced ACh release between the ANT and POST groups (Fig. 2, right). In contrast, the level of ischaemia-induced ACh release was much lower in the RV group than in the POST group. These results suggest that the energy depletion during ischaemia might be less severe or delayed in the right ventricle compared to that in the left ventricle.

Similar to the ouabain-induced NA release, there were no significant differences in the levels of ouabain-induced ACh release among the ANT, POST, and RV groups (Fig. 3, bottom). In a histological study of the human heart (Kawano et al., 2003), the number of acetylcholine esterase (AChE)-positive nerves in the right ventricle is 1.2 times greater than that in the left ventricle, and the number of AChE-positive nerves in the posterior wall is 1.4 times greater than that in the anterior wall of the left ventricle. In the guinea pig heart, the level of choline acetyltransferase activity was approximately two times higher in the right ventricle than in the left ventricle (Schmid et al., 1978). Notwithstanding the discrepancies among reports, these histochemical studies indicate that the number of the vagal nerve terminals in the right ventricle is not less than that in the left ventricle. In other words, the regional difference in the vagal efferent nerve distribution may not account for the lower level of ischaemia-induced ACh release in the RV group as compared with the POST group.

3.3. Pathological significance

The pathological significance of the NA and ACh releases in the ischaemic region is still to be explored. Although high levels of NA reveal cardiotoxicity (Rona, 1985), depletion of catecholamine in reserpinized animals fails to reduce the myocardial infarct size (Toombs et al., 1993; Vander Heide et al., 1995). However, in the reserpinized animals, not only the ischaemic area but also the non-ischaemic area is subjected to catecholamine depletion, making the interpretation of the results difficult. Acetylcholine, when administered prior to coronary occlusion, induces an ischaemic preconditioning mimetic effect (Qin et al., 2002). Acetylcholine also exerts protection on myocytes against hypoxia (Kakinuma et al., 2005). Generally speaking, the excess NA might be harmful whereas the presence of ACh might be beneficial to the myocardium.

One possible feature of the cardiac microdialysis may be that it can monitor the time course of changes in myocardial interstitial NA and ACh levels (Shindo et al., 1996; Kawada et al., 2000; Lameris et al., 2000). Although myocardial ischaemia evokes both the NA and ACh releases, the ACh release is more prompt compared to the NA release. When calculating the percentage against the respective maximum level, the mean NA levels were only 3 and 2% whereas the mean ACh levels reached 79 and 53% in the ANT and POST groups, respectively, during the 0–15 min of the ischaemic period (Fig. 1, note the logarithmic scaling in the top panel). In the RV group, the mean NA level was 28% whereas the mean ACh level reached 72% during the 0–15 min of the ischaemic period. It seems that the ACh release is a protective mechanism against a forthcoming excess of NA in the ischaemic region. Further studies are required to elucidate the significance of a local neuronal environment in modifying the severity of myocardial ischaemia.

3.4. Regional difference in the reflex effects

In the ischaemia protocol, the reflexes from the heart and the arterial baroreflex might have modified the efferent nerve activities. Both the ANT and POST groups showed a significant decrease in the heart rate during ischaemia (Table 2), suggesting an increase in the vagal tone and/or a decrease in the sympathetic tone. Because mean arterial pressure was either unchanged (the ANT group) or decreased (the POST group) (Table 1), the baroreflex cannot account for the decrease in the heart rate during ischaemia. The decreased mean arterial pressure in the POST group compared to the unchanged mean arterial pressure in the ANT group suggests that the cardiodepressor reflex was stronger in the POST than

the ANT group. These differences, however, did not cause the difference in the maximum levels of ischaemia-induced NA and ACh releases between the ANT and POST groups (Fig. 2). Because local release mechanisms became predominant as the ischaemic period is prolonged (Akiyama and Yamazaki, 1999; Kawada et al., 2000, 2006a; Lameris et al., 2000), the difference in the efferent nerve activities might not have affected the maximum levels of NA and ACh releases significantly. In contrast to the ANT and POST groups, the RV group did not show significant changes in mean arterial pressure or the heart rate, suggesting that the effect of RCA occlusion on the systemic haemodynamics was minimal in the present study. Despite the absence of significant bradycardia, the myocardial interstitial ACh level was significantly increased in the RV group during ischaemia, suggesting the involvement of a local release mechanism.

There are limitations to the present study. First, we could not examine regional differences in the NA and ACh releases along the transmural axis from the epicardial layer to the endocardial layer, because we could not control the exact depth of the dialysis fibre implanted transversely in the ventricular wall. Second, species differences should be taken into account when interpreting the present data. As an example, we usually observed a bradycardic response not only during LCX occlusion but also during LAD occlusion in cats (Table 2). In contrast, LAD occlusion in dogs more frequently evokes tachycardia and hypertension (Thames et al., 1978; Zipes, 1990).

4. Conclusion

The maximum levels of ischaemia-induced NA and ACh releases did not differ between the ANT and POST groups but were significantly lower in the RV group. In contrast, myocardial interstitial NA and ACh releases in response to a local administration of ouabain did not show regional differences among the ANT, POST, and RV groups. The regional difference in the ischaemic effects, rather than the regional difference in the functional distributions of sympathetic and vagal efferent nerve terminals, might contribute to the lower levels of ischaemia-induced NA and ACh releases in the RV group.

Acknowledgments

This study was supported by "Health and Labour Sciences Research Grant for Research on Advanced Medical Technology", "Health and Labour Sciences Research Grant for Research on Medical Devices for Analyzing, Supporting and Substituting the Function of Human Body", and "Health and Labour Sciences Research Grant H18-Iryo-Ippan-023" from the Ministry of Health, Labour and Welfare of Japan.

References

Akiyama, T., Yamazaki, T., 1999. Norepinephrine release from cardiac sympathetic nerve endings in the in vivo ischemic region. J. Cardiovasc. Pharmacol. 34, S11–S14.

Akiyama, T., Yamazaki, T., Ninomiya, I., 1991. In vivo monitoring of myocardial interstitial norepinephrine by dialysis technique. Am. J. Physiol, Heart Circ. Physiol. 261, H1643–H1647.

Akiyama, T., Yamazaki, T., Ninomiya, I., 1994. In vivo detection of endogenous acetylcholine release in cat ventricles. Am. J. Physiol, Heart Circ. Physiol. 266, H854–H860.

Armour, J.A., 1999. Myocardial ischaemia and the cardiac nervous system. Cardiovasc. Res. 41, 41–54.

Elvan, A., Zipes, D.P., 1998. Right ventricular infarction causes heterogeneous autonomic denervation of the viable peri-infarct area. Circulation 97, 484–492.

Glantz, S.A., 2002. Primer of Biostatistics, 5th ed. McGraw-Hill, New York.

Hainsworth, R., 1991. Reflexes from the heart. Physiol. Rev. 71, 617–658.

Kakinuma, Y., Ando, M., Kuwabara, M., Katare, R.G., Okudela, K., Kobayashi, M., Sato, T., 2005. Acetylcholine from vagal stimulation protects cardiomyocytes against ischemia and hypoxia involving additive non-hypoxic induction of HIF-1alpha. FEBS Lett. 579, 2111–2118.

Kawada, T., Yamazaki, T., Akiyama, T., Sato, T., Shishido, T., Inagaki, M., Takaki, M., Sugimachi, M., Sunagawa, K., 2000. Differential acetylcholine release mechanisms in the ischemic and non-ischemic myocardium. J. Mol. Cell Cardiol. 32, 405–414.

Kawada, T., Yamazaki, T., Akiyama, T., Shishido, T., Inagaki, M., Uemura, K., Miyamoto, T., Sugimachi, M., Takaki, H., Sunagawa, K., 2001. In vivo assessment of acetylcholine-releasing function at cardiac vagal nerve terminals. Am. J. Physiol, Heart Circ. Physiol. 281, H139–H145.

Kawada, T., Yamazaki, T., Akiyama, T., Mori, H., Uemura, K., Miyamoto, T., Sugimachi, M., Sunagawa, K., 2002. Disruption of vagal efferent axon and nerve terminal function in the postischemic myocardium. Am. J. Physiol, Heart Circ. Physiol. 283, H2687–H2691.

Kawada, T., Yamazaki, T., Akiyama, T., Li, M., Ariumi, H., Mori, H., Sunagawa, K., Sugimachi, M., 2006a. Vagal stimulation suppresses ischemia-induced myocardial interstitial norepinephrine release. Life Sci. 78, 882–887.

Kawada, T., Yamazaki, T., Akiyama, T., Uemura, K., Kamiya, A., Shishido, T., Mori, H., Sugimachi, M., 2006b. Effects of Ca^{2+} channel antagonists on nerve stimulation-induced and ischemia-induced myocardial interstitial acetylcholine release in cats. Am. J. Physiol, Heart Circ. Physiol. 291, H2187–H2191.

Kawano, H., Okada, R., Yano, K., 2003. Histological study on the distribution of autonomic nerves in the human heart. Heart Vessels 18, 32–39.

Kusachi, S., Nishiyama, O., Yasuhara, K., Saito, D., Haraoka, S., Nagashima, H., 1982. Right and left ventricular oxygen metabolism in open-chest dogs. Am. J. Physiol, Heart Circ. Physiol. 243, H761–H766.

Lameris, T.W., de Zeeuw, S., Alberts, G., Boomsma, F., Duncker, D.J., Verdouw, P.D., Veld, A.J., van Den Meiracker, A.H., 2000. Time course and mechanism of myocardial catecholamine release during transient ischemia in vivo. Circulation 101, 2645–2650.

Pierpont, G.L., DeMaster, E.G., Cohn, J.N., 1984. Regional differences in adrenergic function within the left ventricle. Am. J. Physiol, Heart Circ. Physiol. 246, H824–H829.

Qin, Q., Downey, J.M., Cohen, M.V., 2002. Acetylcholine but not adenosine triggers preconditioning through PI3-kinase and a tyrosine kinase. Am. J. Physiol, Heart Circ. Physiol. 284, H727–H734.

Rona, G., 1985. Catecholamine cardiotoxicity. J. Mol. Cell Cardiol. 17, 291–306.

Schömig, A., Dart, A.M., Dietz, R., Mayer, E., Kübler, W., 1984. Release of endogenous catecholamines in the ischemic myocardium of the rat Part. A: locally mediated release. Circ. Res. 55, 689–701.

Schömig, A., Kurz, T., Richardt, G., Schömig, E., 1988. Neuronal sodium homeostasis and axoplasmic amine concentration determine calcium-independent noradrenaline release in normoxic and ischemic rat heart. Circ. Res. 63, 214–226.

Schmid, P.G., Greif, B.J., Lund, D.D., Roskoski Jr., R., 1978. Regional choline acetyltransferase activity in the guinea pig heart. Circ. Res. 42, 657–660.

Schwartz, J.H., 2000. Neurotransmitters. In: Kandel, E.R., Schwartz, J.H., Jessell, T.M. (Eds.), Principles of Neural Science, 4th ed. McGraw-Hill, New York, pp. 280–297.

Shindo, T., Akiyama, T., Yamazaki, T., Ninomiya, I., 1996. Regional myocardial interstitial norepinephrine kinetics during coronary occlusion and reperfusion. Am. J. Physiol, Heart Circ. Physiol. 270, H245–H251.

Thames, M.D., Klopfenstein, H.S., Abboud, F.M., Mark, A.L., Walker, J.L., 1978. Preferential distribution of inhibitory cardiac receptors with vagal afferents to the inferoposterior wall of the left ventricle activated during coronary occlusion in the dog. Circ. Res. 43, 512–519.

Toombs, C.F., Wiltse, A.L., Shebuski, R.J., 1993. Ischemic preconditioning fails to limit infarct size in reserpinized rabbit myocardium. Implication of norepinephrine release in the preconditioning effect. Circulation 88, 2351–2358.

Vander Heide, R.S., Schwartz, L.M., Jennings, R.B., Reimer, K.A., 1995. Effect of catecholamine depletion on myocardial infarct size in dogs: role of catecholamines in ischemic preconditioning. Cardiovasc. Res. 30, 656–662.

Walker, J.L., Thames, M.D., Abboud, F.M., Mark, A.L., Klopfenstein, H.S., 1978. Preferential distribution of inhibitory cardiac receptors in left ventricle of the dog. Am. J. Physiol, Heart Circ. Physiol. 235, H188–H192.

Weiss, H.R., Neubauer, J.A., Lipp, J.A., Shinha, A.K., 1978. Quantitative determination of regional oxygen consumption in the dog heart. Circ. Res. 42, 394–401.

Yamazaki, T., Akiyama, T., Kitagawa, H., Takauchi, Y., Kawada, T., Sunagawa, K., 1997. A new, concise dialysis approach to assessment of cardiac sympathetic nerve terminal abnormalities. Am. J. Physiol, Heart Circ. Physiol. 272, H1182–H1187.

Yamazaki, T., Akiyama, T., Kawada, T., 1999. Effects of ouabain on in situ cardiac sympathetic nerve endings. Neurochem. Int. 35, 439–445.

Zipes, D.P., 1990. Influence of myocardial ischemia and infarction on autonomic innervation of heart. Circulation 82, 1095–1105.